Biochimica et Biophysica Acta 1863 (2016) 544–561

Contents lists available at ScienceDirect

Biochimica et Biophysica Acta

journal homepage: www.elsevier.com/locate/bbamcr

The signaling module cAMP/Epac/Rap1/PLCε/IP_3 mobilizes acrosomal calcium during sperm exocytosis

Ornella Lucchesi, María C. Ruete, Matías A. Bustos [1], María F. Quevedo, Claudia N. Tomes *

Laboratorio de Biología Celular y Molecular, Instituto de Histología y Embriología, IHEM-CONICET, Facultad de Ciencias Médicas, Universidad Nacional de Cuyo, Mendoza 5500, Argentina

ARTICLE INFO

Article history:
Received 1 August 2015
Received in revised form 23 November 2015
Accepted 14 December 2015
Available online 17 December 2015

Keywords:
Acrosome reaction
Calcium
TAT-cAMP sponge
Epac
Exocytosis
Protein transduction

ABSTRACT

Exocytosis of the sperm's single secretory granule, or acrosome, is a regulated exocytosis triggered by components of the egg's investments. In addition to external calcium, sperm exocytosis (termed the acrosome reaction) requires cAMP synthesized endogenously and calcium mobilized from the acrosome through IP_3-sensitive channels. The relevant cAMP target is Epac. In the first part of this paper, we present a novel tool (the TAT-cAMP sponge) to investigate cAMP-related signaling pathways in response to progesterone as acrosome reaction trigger. The TAT-cAMP sponge consists of the cAMP-binding sites of protein kinase A regulatory subunit RIβ fused to the protein transduction domain TAT of the human immunodeficiency virus-1. The sponge permeated into sperm, sequestered endogenous cAMP, and blocked exocytosis. Progesterone increased the population of sperm with Rap1-GTP, Rab3-GTP, and Rab27-GTP in the acrosomal region; pretreatment with the TAT-cAMP sponge prevented the activation of all three GTPases. In the second part of this manuscript, we show that phospholipase Cε (PLCε) is required for the acrosome reaction downstream of Rap1 and upstream of intra-acrosomal calcium mobilization. Last, we present direct evidence that cAMP, Epac, Rap1, and PLCε are necessary for calcium mobilization from sperm's secretory granule. In summary, we describe here a pathway that connects cAMP to calcium mobilization from the acrosome during sperm exocytosis. Never before had direct evidence for each step of the cascade been put together in the same study.

1. Introduction

Cyclic adenosine monophosphate (cAMP) is a central second messenger that controls a plethora of vital functions. The strategies used to attribute cellular responses to cAMP typically rely on increasing cAMP levels with membrane-permeant analogs, phosphodiesterase inhibitors, and/or protein G/adenylyl cyclase stimulators. While these strategies have been fruitful, the irrefutable proof that a mechanism is mediated by cAMP can only be achieved if the said mechanism/cellular response is abolished when endogenous cAMP is unavailable. To the best of our knowledge, only two strategies have been designed to deplete cells of cAMP. One of them consists of introducing a phosphodiesterase in permeabilized cells to digest cAMP [9]. The other applies a genetically encoded buffer (named cAMP sponge) based on the high-affinity cAMP-binding sites of the regulatory subunit of the cAMP-dependent protein kinase (PKA) to deplete cAMP from the cytosol of transfected cells [33].

Exocytosis of the acrosome, or acrosome reaction (AR), is a regulated secretion event that sperm must undergo in order to fertilize the egg. Each sperm contains a single, very large, and electron dense acrosome that, in response to exocytosis inducers, first swells to contact the cell membrane, second becomes attached to and fuses with it and third sheds entirely, together with the portion of plasma membrane that surrounds it. These events are coupled to complex calcium signaling. Typically, AR triggers evoke a transient influx of calcium into the cytosol through plasma membrane channels; this event initiates complex signaling cascades that lead to intracellular calcium mobilization. Emptying of intracellular reservoires causes the opening of store operated calcium channels in the plasma membrane that elicits a sustained calcium signal. An influx of external calcium into sperm driven by calcium ionophores resembles the latter and induces the AR. So does the addition of $CaCl_2$ to cells with their plasma membrane permeabilized with

Abbreviations: 2-APB, 2-aminoethoxydiphenylborate; AR, acrosome reaction; 6-Bnz-cAMP, N^6-benzoyladenosine-3′,5′-cyclic monophosphate; cAMP, cyclic adenosine monophosphate; Epac, guanine nucleotide exchange factor activated by cAMP; GEF, guanine nucleotide exchange factor; GST, glutathione-S-transferase; HTF, human tubal fluid; IP_3, 1,4,5-trisphosphate; IPTG, isopropyl-β-D-thio-galactoside; NP-EGTA-AM, *O*-nitrophenyl EGTA-acetoxymethyl ester; PBS, phosphate-buffered saline; 8-pCPT-2′-*O*-Me-cAMP, 8-(*p*-chlorophenylthio)-2 prime-*O*-methyladenosine-3′,5′-cyclic monophosphate; PKA, cAMP-dependent protein kinase; PLC, phospholipase C; PVP, polyvinylpyrrolidone; sAC, soluble adenylyl cylase; SDS–PAGE, sodium dodecyl sulfate–polyacrylamide gel electrophoresis; Slac2-b, synaptotagmin-like protein homology domain; SLO, streptolysin O.

* Corresponding author at: Instituto de Histología y Embriología (IHEM, CONICET/UNCuyo), Facultad de Ciencias Médicas, CC56, Universidad Nacional de Cuyo, Mendoza 5500, Argentina.
E-mail address: ctomes@fcm.uncu.edu.ar (C.N. Tomes).
[1] Current address: Department of Molecular Oncology, John Wayne Cancer Institute, Santa Monica, California 90404, United States.

http://dx.doi.org/10.1016/j.bbamcr.2015.12.007
0167-4889/

toxins such as streptolysin O (SLO [1,26,68]) or perfringolysin O [42]. In the first part of this paper, we describe a permeable, recombinant version of the cAMP sponge that we introduced into live human sperm through a mechanism known as protein transduction. Thanks to this tool, we demonstrate that AR triggers require cAMP to induce swelling of the acrosome and to activate pathways that mobilize calcium from the intra-acrosomal pool. In particular, relevant for sperm biologists are the observations that progesterone requires cAMP to achieve the AR and the elucidation of the signal transduction pathways involved in the exocytotic response to this hormone.

In certain neurons, neuroendocrine, and exocrine acinar cells, cAMP potentiates calcium-dependent exocytosis, whereas in various non-neuronal cells, cAMP is the principal trigger of regulated secretion [10,54,58]. Until not too long ago, it was thought that the effects of cAMP in regulated exocytosis were mediated by PKA through phosphorylation of relevant substrates. More recently, we learned that cAMP modulates exocytosis via PKA-dependent and/or PKA-independent mechanisms. The latter are mediated by guanine nucleotide exchange factors (GEFs) activated by cAMP (Epacs, reviewed by [6,12,22,32,53]). Many processes of stimulus-secretion coupling are regulated by both Epac and PKA; how do they cross talk is still an open question. In sperm, the Epac-selective cAMP analog 8-(*p*-chlorophenylthio)-2 prime-*O*-methyladenosine-3′,5′-cyclic monophosphate (8-pCPT-2′-*O*-Me-cAMP) induces exocytosis per se, while the PKA-selective analog N^6-benzoyladenosine-3′,5′-cyclic monophosphate (6-Bnz-cAMP) does not [8]. Furthermore, calcium-induced AR in SLO-permeabilized human sperm is mediated by cAMP/Epac and independent of PKA [9].

Epac proteins consist of a carboxyl-terminal catalytic region and an amino-terminal regulatory region, which harbors one cAMP-binding domain in Epac1 and two in Epac2 [22,32,51]. In the absence of cAMP, the regulatory region covers the CDC25-homology domain and autoinhibits Epac's enzymatic activity by hindering the access of its substrates to the catalytic site [6,7,45]. Upon binding of cAMP, a subtle conformational change allows the regulatory region to move away, lifting the autoinhibition [5,22]. Epac's catalytic portion bears a GEF activity specific for Rap1 and Rap2 [17,29]. The small GTPase Rap1 is necessary to achieve acrosomal exocytosis [8,35,47]. Importantly, Rap1 exchanges GDP for GTP in response to calcium and 8-pCPT-2′-*O*-Me-cAMP [2,8,38,47]. One of the advances reported here is that progesterone, perhaps the most widely used AR inducer, increases the population of cells with active Rap1 in the acrosomal region. Equally important is the finding that progesterone requires cAMP but not PKA to activate Rap1.

In many models, cAMP/PKA and/or cAMP/Epac facilitate the opening of calcium release channels located in intracellular stores. Metabolites such as inositol 1,4,5-trisphosphate (IP_3), cyclic ADP-ribose (the proposed endogenous ligand for ryanodine receptors), and NAADP enhance the ability of cytosolic calcium to activate various calcium release channels located on intracellular organelles [30,32]. Pharmacological blocking of these pathways impairs glucose-induced insulin secretion, indicating that intracellular calcium is required for exocytosis [39]. What could be the link between cAMP/Epac and intracellular calcium mobilization in secretory cells? An interesting candidate is PLCε, the only effector recruited/activated by GTP-bound Rap that has been implicated in Epac-mediated secretory responses [18,19]. In sperm, the acrosome itself behaves as an internal calcium store [14,16,43,47,49]. We have previously shown by single-cell confocal microscopy that intra-acrosomal calcium is released through IP_3-sensitive channels because the blocker 2-aminoethoxydiphenylborate (2-APB) prevents – and the agonist adenophostin A elicits – its mobilization [47]. The sensitivity of the AR to these agents provides pharmacological evidence that intracellular calcium is mobilized via IP_3-sensitive channels in human sperm [8,16,35]. One of the significant advances that we describe in this manuscript is that PLCε is required to mobilize calcium from the acrosomal reservoir. The stimulation of sperm's Epac with 8-pCPT-2′-*O*-Me-cAMP suffices to elicit intra-acrosomal calcium efflux through a pathway that involves Rap1 and PLCε.

2. Materials and methods

2.1. Reagents

Recombinant SLO was obtained from Dr. Bhakdi (University of Mainz, Mainz, Germany). The rabbit polyclonal anti-GST (purified IgG) antibodies were purchased from EMD Millipore Corporation (Billerica, MA). The mouse monoclonal anti-His_6 antibody (purified IgG 2a) was from GE Healthcare (Buenos Aires, Argentina). The rabbit polyclonals anti-PLCε1 (affinity purified, catalogue number ARP50613_P050) and anti-PLCγ1 (affinity purified, catalogue number ARP33086_P050) were from Aviva Systems Biol (San Diego, CA). The rabbit polyclonal antibodies against Epac 1/2 were generated by Genemed Synthesis, Inc. (San Francisco, CA) using the synthetic peptide LREDNCHFLRVDK, and affinity purified on immobilized Epac peptide [9]. Anti-Rap 1A/B rabbit polyclonal antibodies were raised against the peptide EDERVVGKEQGQNLC and affinity purified on immobilized peptide (GenScript Corporation, Piscataway, NJ) [8]. The rabbit polyclonal anti-α-tubulin antibody (affinity purified with the immunogen) was from Synaptic Systems (Göttingen, Germany). Horseradish peroxidase-conjugated goat anti-mouse IgG (H + L) was from Kierkegaard & Perry Laboratories, Inc. (Gaithersburg, MD). Horseradish peroxidase- and Cy™3-conjugated goat anti-rabbit as well as Cy™3-conjugated goat anti-mouse IgGs (H + L) were from Jackson ImmunoResearch (West Grove, PA). 8-pCPT-2′-*O*-Me-cAMP and 6-Bnz-cAMP were from Axxora, LLC (San Diego, CA). U73122 (1-(6-((17β-3-methoxyestra-1,3,5(10)-trien-17-yl) amino)hexyl)-1 H-pyrrole-2,5-dione) was from Merck Química Argentina SAIC (Buenos Aires, Argentina). *O*-nitrophenyl EGTA-acetoxymethyl ester (NP-EGTA-AM) and 1-[2-Amino-5-(2,7-dichloro-6-hydroxy-3-oxo-9-xanthenyl) phenoxy]-2-(2-amino-5-methylphenoxy)ethane-*N*,*N*,*N*′,*N*′-tetraacetic acid, pentaacetoxymethyl ester (Fluo3-AM) were purchased from Life Technologies (Buenos Aires, Argentina). Prestained molecular weight markers were from Boston BioProducts Inc. (Worcester, MA). H89 (*N*-[2-(p-bromocinnamylamino)ethyl]-5-isoquinolinesulfonamide) and KH7 were purchased from R&D Systems (Minneapolis, MN). Adenophostin A, hexasodium salt, and 2-APB from Calbiochem were purchased from Merck Química Argentina S.A.I.C. (Buenos Aires, Argentina). Glutathione–Sepharose and Ni-NTA-agarose were from GE Healthcare. All other chemicals were purchased from Sigma-Aldrich™ Argentina S.A., Genbiotech, or Tecnolab (Buenos Aires, Argentina).

2.2. Expression and purification of recombinant proteins

An expression plasmid pQE80L (Qiagen, Valencia, CA) containing the cDNA encoding a membrane-permeant version of human Rab3A bearing a Q81L point mutation fused to His_6 (R-Rab3A, [34]) was generously provided by Dr. C. López (Cuyo University, Mendoza, Argentina). GST fusion protein with the Rab3-GTP-binding domain of rat RIM (amino acids 11–398, RIM-RBD) [13] in a pGEX2p vector was generously provided by Dr. R. Regazzi (University of Lausanne, Lausanne, Switzerland). The Rap-GTP-binding cassette Ral-GDS-RBD fused to GST [63] was a kind gift from Dr. O. Coso (Universidad de Buenos Aires, Buenos Aires, Argentina). DNA encoding the Rab27-GTP-binding domain of Slac2-b (synaptotagmin-like protein homology domain; amino acids 1–79) in pGEX-2 T [31] was a kind gift from Dr. R. Shirakawa (Kyoto University, Kyoto, Japan). The cDNA encoding the light chain of botulinum toxin B fused to His_6 (pQE3, Qiagen) was generously provided by Dr. T. Binz (Medizinische Hochschule Hannover, Hannover, Germany).

The cDNA-encoding R-Rab3A was transformed into *Escherichia coli* BL21(DE3) $T1^R$ and expression of the recombinant protein was accomplished by incubation with 0.5 mM isopropyl-β-D-thio-galactoside (IPTG) for 3 h at 37 °C. R-Rab3A was geranylgeranylated and loaded with GTP-γ-S as described [11]. The plasmid construct encoding botulinum toxin B was transformed into *E. coli* M15pRep4 (Qiagen) and

protein expression was induced 4 h at 30 °C with 1 mM IPTG. Plasmids enconding all GST-fused proteins were transformed in *E. coli* BL21(DE3) $T1^R$, and protein expression was induced with IPTG as follows: GST-Slac2-b-SHD, 0.5 mM IPTG for 3 h at 37 °C; GST-Ral-GDS-RBD 0.1 mM IPTG, overnight at 22 °C; GST-RIM-RBD 0.5 mM IPTG, overnight at 22 °C. GST-fused recombinant proteins were purified on glutathione–Sepharose beads following standard procedures. The purification of His_6-tagged recombinant proteins was carried out under native conditions according to Qiagen's instructions except that the purification buffers contained 20 mM Tris–HCl, pH 7.4, and 200 mM NaCl; lysis buffer contained 10 mM imidazole, washing buffer contained 50 mM imidazole, and elution buffer contained 250 mM imidazole. Recombinant protein concentrations were determined by the Bradford method (BioRad) using bovine serum albumin as a standard in 96-well microplates and quantified on a BioRad 3550 Microplate Reader or from the intensities of the bands in Coomassie blue-stained sodium dodecyl sulfate (SDS)–polyacrylamide electrophoresis (SDS–PAGE) gels.

2.3. Construction and expression of the TAT-cAMP sponge

The cDNA encoding a permeable version of the cAMP sponge [33] was synthesized by Genscript. Briefly, the DNA encoding amino acids 132 to 381 of the human PKA regulatory subunit I β was optimized for bacterial expression. The insert was subcloned in frame with the TAT sequence of HIV virus (RKKRRQRRR) for protein transduction into the *Hin*dIII–*Bam*HI cloning site of pET28a(+) vector (Novagen, now Merck-Millipore). The cDNA-encoding His_6-TAT-cAMP sponge was transformed into *E. coli* BL21(DE3) $T1^R$ (Stratagene, La Jolla, CA), and the expression of recombinant protein was accomplished by incubation with 0.5 mM IPTG overnight at 22 °C. The purification of the TAT-cAMP sponge was carried out following standard procedures.

2.4. Human sperm sample preparation procedures

Human semen samples were obtained from normal healthy donors. Semen was allowed to liquefy for 30–60 min at 37 °C. Following a swim-up protocol to isolate highly motile cells, sperm concentrations were adjusted to 10^7/ml before incubating for at least 2 h under capacitating conditions [Human Tubal Fluid media as formulated by Irvine Scientific (Santa Ana, CA) supplemented with 0.5% bovine serum albumin (BSA), HTF medium), 37 °C, 5% CO_2/95% air]. Samples were processed for AR assays, immunofluorescence, Western blot, transmission electron microscopy, and single-cell calcium imaging.

2.5. Trypsin protection assay for the TAT-cAMP sponge transduced into human sperm

Capacitated sperm suspended in HTF medium were washed and resuspended (5×10^5 cells in 50 μl for immunofluorescence, 2×10^6 cells in 200 μl for Western blot) in HTF (without BSA) and incubated with 1 μM TAT-cAMP sponge for 15 min at 37 °C. After washing once with the same medium, sperm were exposed to 0.1 or 1 μg/ml trypsin (Sigma) for 20 min at 37 °C. Cells were washed and processed for conventional immunofluorescence or Western blot with anti-His_6 antibodies as probe to detect the internalized sponge.

2.6. SDS–PAGE and Western blot

Cells were washed twice with PBS, lysed in cold 20 mM Tris–HCl, pH 7.5, 150 mM NaCl, 10% glycerol, 1% Triton X-100, 5 mM $MgCl_2$, and a protease inhibitor cocktail (P2714, Sigma). Sperm were sonicated (3 × 15 s), and proteins were allowed to diffuse into the lysis buffer for 30 min at 4 °C. Whole-cell detergent extracts were clarified by centrifugation at 14,000 × *g* for 20 min. Proteins extracted from sperm and those recovered from the supernantant were precipitated with CCl_3H-CH_3OH-H_2O. Precipitated proteins were dissolved in sample buffer by heating once at 60 °C for 10 min and once at 95 °C for 3 min.

Proteins were separated on polyacrylamide slab gels and transferred to 0.22 μm nitrocellulose membranes (Hybond, GE Healthcare). Non-specific reactivity was blocked by incubation for 1 h at room temperature with 3% skim milk dissolved in washing buffer (PBS pH 7.6, 0.1% Tween 20). Blots were incubated with anti-His_6 and anti-α-tubulin antibodies (0.2 μg/ml in washing buffer) for 2 h at room temperature or overnight at 4 °C. Horseradish peroxidase-conjugated goat anti-mouse (for detection of anti-His_6 antibodies) or anti-rabbit (for detection of anti-α tubulin antibodies) IgGs were used as secondary antibodies (0.1 μg/ml) with 1 h incubations. Excess first and second antibodies were removed by washing 5 × 7 min in washing buffer. Detection was accomplished with a chemiluminescence system from Millipore (WBKLS, Biopore, Buenos Aires, Argentina) on a Luminescent Image Analyzer LAS-4000 (Fujifilm, Tokyo, Japan).

2.7. AR assays

For experiments involving intact sperm, we aliquoted capacitated sperm suspended in HTF, added the reagents to test followed by 10 μM A23187, 15 μM progesterone, 300 nM R-Rab3A, or 50 μM 8-pCPT-2′-*O*-Me-cAMP and incubated for 10–15 min at 37 °C after each addition. For experiments involving permeabilized cells, sperm were washed twice with PBS and resuspended in cold PBS containing 3 U/ml SLO for 15 min at 4 °C. Cells were washed once with PBS and resuspended in ice-cold sucrose buffer (250 mM sucrose, 0.5 mM EGTA, 20 mM Hepes-K, pH 7) containing 2 mM DTT. We added inhibitors and stimulants sequentially as indicated in the figure legends, and incubated for 8–15 min at 37 °C after each addition. When indicated, we preloaded SLO-permeabilized sperm with photosensitive NP-EGTA-AM for 10 min at 37 °C before incubating in the presence of inhibitors and/or calcium, carrying out all procedures in the dark. Photolysis was induced after the last incubation by exposing twice (1 min each time) to a UV transilluminator (FBTIV-614, Fisher Scientific, Pittsburgh, PA), mixing, and incubating for 5 min at 37 °C. Sperm were spotted on Teflon-printed slides, air dried, and fixed/permeabilized in ice-cold methanol for 20 s. An alternatively fixation protocol (described in Section 2.9) rendered identical results. Acrosomal status was evaluated by staining with FITC-coupled *Pisum sativum* agglutinin (FITC-PSA, 25 μg/ml in PBS) for 40 min at room temperature followed by a 20 min-wash in water [37]. We scored at least 200 cells per condition using an upright Nikon Optiphot II microscope equipped with epifluorescence optics. Basal ("control," no stimulation) and positive ("Pg," 15 μM progesterone for non-permeabilized and "calcium," 0.5 mM $CaCl_2$ [corresponding to 10 μM free calcium estimated by MAXCHELATOR, a series of program(s) for determining the free metal concentration in the presence of chelators; available on the World Wide Web at http://www.stanford.edu/~cpatton/maxc.html, Chris Patton, Stanford University, Standord, CA] for SLO-permeabilized) controls were included in all experiments. Acrosomal exocytosis indices were calculated by subtracting the number of spontaneously reacted spermatozoa (basal control without stimulation, ranged from ≈5 to 25% before normalization) from all values and expressing the results as a percentage of the AR observed in the positive control (ranged from ≈15 to 60% before normalization; assigned 100% of responsive cells for normalization). We only included in our analysis results derived from experiments that produced similar responses and where the difference between basal and stimulated conditions was of at least 8–10 percentage points. SLO-permeabilized samples with a level of spontaneously reacted sperm higher than 30% were excluded from the analysis. Data were evaluated with the program GraphPad Prism 5 using the Tukey–Kramer post hoc test for pairwise comparisons. Differences were considered significant at the $P < 0.05$ level.

2.8. Conventional indirect immunofluorescence

Sperm (5×10^5 cells) were fixed in 2% paraformaldehyde in PBS for 15 min at room temperature, centrifuged and resuspended in PBS containing 100 mM glycine to neutralize the fixative. Sperm were attached to poly-L-lysine (stock 0.1% *w/v* (Sigma) diluted 1:20 in water)-coated, 12 mm round coverslips by incubating for 30 min at room temperature in a moisturized chamber. Next, we permeabilized the plasma membrane with 0.1% Triton X-100 in PBS for 10 min at room temperature and washed three times with PBS containing 0.1% polyvinylpyrrolidone

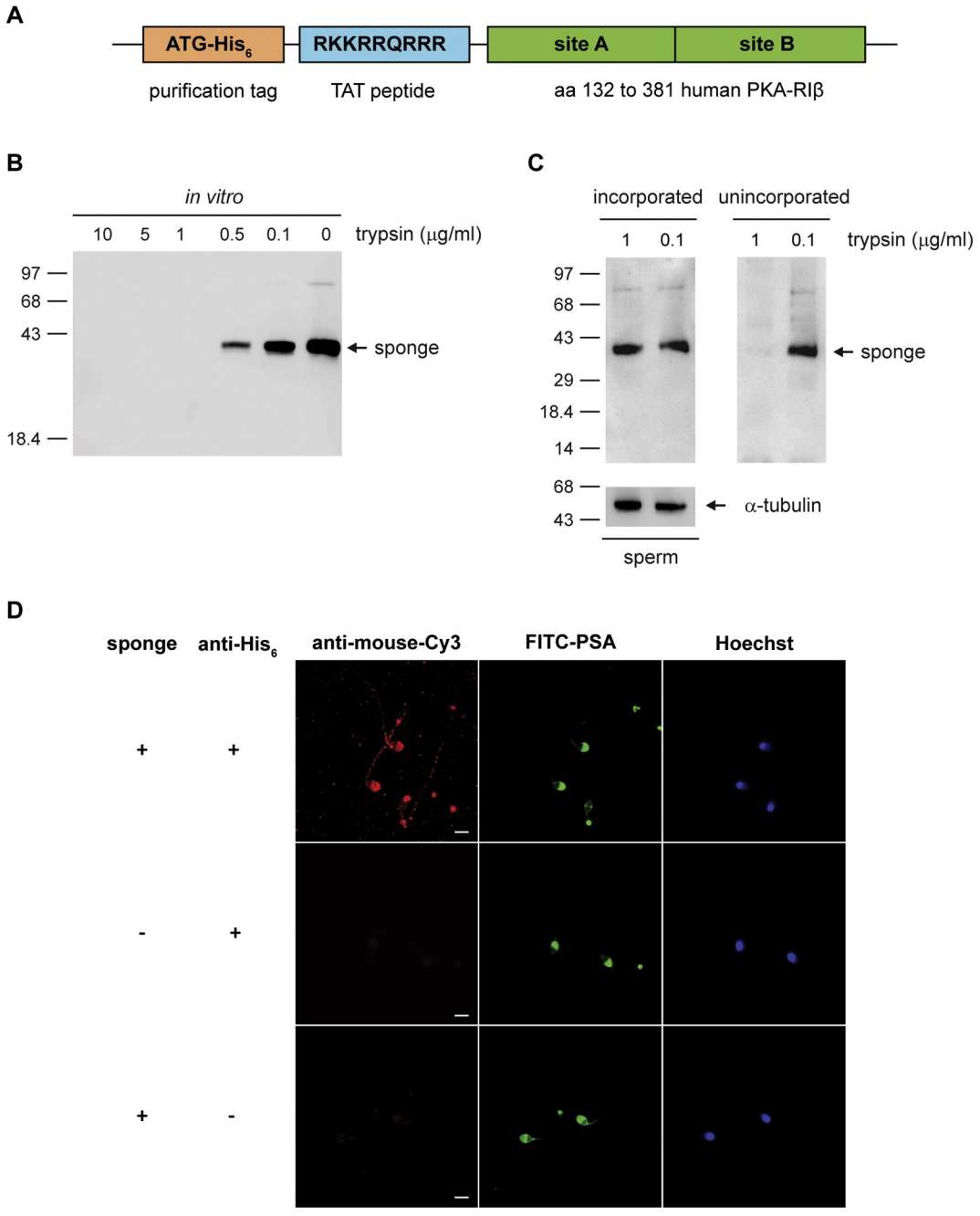

Fig. 1. The TAT-cAMP sponge transduces into human sperm. (A) Schematic representation of the TAT-sponge. The carboxy-terminus of PKA-RIβ (amino acids 132–381) containing its two cAMP-binding sites (green) was fused at its N-terminus to the TAT peptide from HIV virus (blue) for protein transduction and a His_6 tag (orange) for affinity purification and immunodetection. (B) Trypsin sensitivity of the TAT-sponge in solution; 720 ng (1 μM) of the sponge was incubated with trypsin for 20 min at 37 °C. Samples were electrophoresed on 10% Tris–tricine–SDS–polyacrylamide gels, transferred to nitrocellulose, and immunoblotted with the anti-His_6 antibody. Mr standards ($\times 10^3$) are indicated on the left. Shown is an experiment representative of two repetitions. (C) The sponge was delivered to the intracellular compartment of human sperm because it resisted degradation by trypsin. Capacitated human sperm were incubated with 1 μM TAT-sponge for 20 min at 37 °C. Subsequently, cells were treated with trypsin. After 20 min at 37 °C, samples were centrifuged and proteins from both the sperm pellet (incorporated) and the extracellular supernatant (unincorporated) were processed for anti-His_6 Western blot. Anti-α-tubulin was used to show equal loads. Mr standards ($\times 10^3$) are indicated on the left. Shown is an experiment representative of two repetitions. (D) Capacitated human sperm incubated first with 1 μM TAT-sponge (top and bottom panels) and second with 1 μg/ml trypsin were processed for anti-His_6 immunofluorescence. The central panels show images from experiments where the primary antibody was omitted (antibody specificity control). Cells were triple stained with a fluorescent anti-mouse antibody as read out for the presence of the sponge (anti-mouse-Cy3, red, left panels), FITC-PSA (to assess the integrity of the acrosome; green, central panels), and Hoechst 33342 (to visualize all cells in the field; blue, right panels). Shown are epifluorescence micrographs of typically stained cells. Bars = 5 μm.

(PVP, average M.W. = 40,000; PBS/PVP). Nonspecific staining was blocked by incubation in 5% bovine serum albumin in PBS/PVP for 1 h at 37 °C. Anti-His_6 antibodies were diluted at 4 μg/ml and anti-PLCε at 10 μg/ml in 3% bovine serum albumin in PBS/PVP, added to the coverslips, and incubated for 1 h at 37 °C in a moisturized chamber. After washing three times, 6 min each with PBS/PVP, we added Cy™3-conjugated anti-rabbit (for detection of anti-PLCε antibodies) or anti-mouse (for detection of anti-His_6 antibodies) IgGs (2.5 μg/ml in 1% bovine serum albumin in PBS/PVP) and incubated for 1 h at room temperature protected from light. Coverslips were washed three times for 6 min with PBS/PVP. Cells were subsequently treated with ice-cold methanol for 30 s and stained for acrosomal contents as described in 2.7 (but without air drying), mounted with Mowiol® 4–88 in PBS containing 2 μM Hoechst 33342 and stored at −20 °C in the dark until examination with an Eclipse TE2000 Nikon microscope equipped with a Plan Apo 40×/1.40 oil objective. Images were captured with a Hamamatsu digital C4742-95 camera operated with MetaMorph 6.1 software (Universal Imaging Corp., USA). Background was subtracted and brightness/contrast were adjusted to render an all-or nothing labeling pattern using Image J (freeware from N.I.H.).

2.9. Detection of GTP-Rab3, GTP-Rab27, and GTP-Rap1 by far-immunofluorescence

Capacitated sperm suspensions were incubated with 100 μM 2-aminoethoxydiphenylborate (2-APB) for 10 min at 37 °C to prevent acrosomal loss due to exocytosis, treated with AR blockers and/or inducers (10–15 min at 37 °C after each addition), fixed, smeared on coverslips, permeabilized, and blocked as described in 2.8. Slides were overlain with 140 nM GST-RIM-RBD, GST-Slac2-b-SHD, or GST-Ral-GDS-RBD in 3% bovine serum albumin in PBS/PVP for 1 h at 37 °C. After washing (three times, 6 min each, PBS/PVP), coverslips were processed as described in Section 2.7 using anti-GST (31.5 μg/ml) as primary antibodies. We scored the presence of immunostaining in the acrosomal region by manually counting between 100 and 200 cells per condition, either directly at the fluorescence microscope. Data were evaluated with the program GraphPad Prism 5 using the Tukey–Kramer post hoc test for pairwise comparisons. Differences were considered significant at the $P < 0.05$ level.

2.10. Single-cell imaging of intra-acrosomal calcium

Capacitated, SLO-permeabilized sperm (250 μl aliquots, 4×10^7 cells) suspended in sucrose buffer were incubated with 100 nM (final concentration) botulinum toxin B (preactivated with 1 mM DTT during 15 min at 37 °C) and then loaded with Fluo3-AM (2 μM final concentration, dispersed with pluronic acid F-127, 0.08% final concentration) at 37 °C for 30 min. Cells were washed once to remove excess dye, resuspended in sucrose buffer and treated or not for 15 min at 37 °C with the AR blockers to test. Twenty-five microliters of each sample was gently introduced into an imaging chamber fitted with a poly-L-lysine-coated 25 mm round coverslip. The chamber was transferred to the microscope stage, washed with sucrose buffer to remove unbound sperm, and replenished with 300 μl fresh sucrose buffer. Cells were maintained at 37 °C at all times. After the baseline was stabilized, 0.5 mM $CaCl_2$, 50 μM 8-pCPT-2′-*O*-Me-cAMP, or 200 μM 6-Bnz-cAMP was added to the medium. A 473 nm laser with an emission of 535 nm was used to generate the excitation for Fluo-3. A Plan Apo 60× objective was used for imaging in an Olympus FV 1000 confocal microscope. Images were collected in every 3 s using the Fluoview FV-1000 software with a total recording time of 300 s (30 s before and 270 s after addition of the inducers). Cells that came out of focus because they moved or those with uneven or no dye loading were excluded from the analysis. Fluorescence measurements in individual sperm were made by manually drawing a region of interest around the acrosome and midpiece of each cell after subtracting background noise. Results are presented as pseudo color $[Ca^{2+}]$ of 10 images collected in every 30 s. Raw intensity values were imported into Microsoft Excel and normalized using F/F_o ratios after background subtraction, where F is fluorescence intensity at time t and F_o is the baseline as calculated by averaging the 10 frames before addition of the stimuli. Cells with peak changes of >50% in F/F_o after application of $CaCl_2$ or 8-pCPT-2′-*O*-Me-cAMP were counted as responsive. The total series of F/F_o are plotted versus time. Relative fluorescence (%) is the fluorescence normalized to that obtained before the addition of $CaCl_2$ or 8-pCPT-2-O′-Me-cAMP. Experiments were carried out three times, each repeat on a different sample. Data were plotted and analyzed with GraphPad Prism 5.

2.11. Transmission electron microscopy

Capacitated human sperm (5×10^6 cells in 200 μl per condition) were incubated with 100 nM TAT-cAMP sponge, 10 μM KH7, or 20 μM BAPTA-AM for 15 min at 37 °C and subsequently challenged with 10 μM A23187 or 15 μM progesterone during 15 min at 37 °C. We then added 1.6 mM tannic acid and incubated for 5 min at 37 °C. Afterward, sperm suspensions were fixed in 2.5% glutaraldehyde in HTF overnight at 4 °C. Fixed sperm samples were washed twice in PBS (20 min at 4 °C each) and postfixed in 1% osmium tetroxide in PBS for 2 h at room temperature, washed three times in PBS (20 min at 4 °C each), and dehydrated sequentially with increasing concentrations of ice-cold acetone (twice with 50% for 5 min, once with 70%, once with 80%, and once with 95%, all for 15 min, and three times with 100% for 15 min at room temperature). Cells were infiltrated in 1:1 acetone:Spurr (a low-viscosity epoxy resin embedding medium) overnight at room temperature and finally embedded in fresh pure resin overnight at room temperature. Samples were cured 24 h at 70 °C and processed at an Academic facility (Facultad de Ciencias Veterinarias, Universidad Nacional de La Plata, La Plata, Argentina) where thin sections were cut, collected on 200-mesh copper grids, and stained with saturated uranyl acetate in methanol plus lead citrate. Grids were observed and photographed in a Zeiss 902 electron

Fig. 2. Progesterone and A23187 require endogenous cAMP to achieve acrosomal swelling and the AR. Capacitated human sperm were exposed to increasing concentrations of the TAT-cAMP sponge for 15 min at 37 °C. Acrosomal exocytosis was initiated with 15 μM progesterone (A) or 10 μM A23187 (B) and incubating at 37 °C for a further 15 min. (C) 100 nM TAT-cAMP sponge (sp) was preincubated with 200 nM 6-Bnz-cAMP (6-Bnz) for 15 min at 37 °C before introducing it into sperm as in A. The AR was elicited by adding 15 μM progesterone (Pg) or 50 μM 8-pCPT-2′-*O*-Me-cAMP (8-pCPT) and incubating for 15 min at 37 °C (black bars). Controls (gray bars) include: background AR in the absence of any stimulation (control); AR stimulated by 15 μM progesterone (Pg) or 50 μM 8-pCPT-2′-*O*-Me-cAMP (8-pCPT); inhibition by 100 nM TAT-cAMP sponge (sp → Pg); lack of effect of 200 nM 6-Bnz-cAMP alone (6-Bnz) or mixed with 100 nM TAT-cAMP sponge (sp + 6-Bnz). Different letters indicate statistical significance ($P < 0.001$). (D) Capacitated human sperm were incubated with 100 nM TAT-cAMP sponge (sp) for 15 min at 37 °C. Acrosomal exocytosis was initiated by adding 300 nM R-Rab3A geranylgeranylated and loaded with GTP-γ-S (R-Rab3A) and incubating at 37 °C for a further 15 min (black bar). Controls (gray bars) are the same as in C, plus the AR stimulated by 300 nM active R-Rab3A. Different letters indicate statistical significance ($P < 0.01$). (A–D) Sperm were fixed and the AR was measured by FITC-PSA binding as described in Section 2.7. "AR assays". The data represent the mean ± SEM of at least three independent experiments. (E–H) Capacitated human sperm were treated for 15 min at 37 °C with 100 nM TAT-cAMP sponge (Ec, Gc) or 10 μM KH7 (Ed, Gd) before challenging with 15 μM progesterone (Eb-d) or 10 μM A23187 (Gb-d) and incubating as before. The following two controls were conducted in parallel: (Ea, Ga) untreated cells as control for the morphology of unswollen, undocked acrosomes; (Eb, Gb) 20 μM BAPTA-AM followed by the inducers as control for the morphology of swollen, docked acrosomes. Shown are transmission electron micrographs of cells typical of each category. (F, H) Quantification of the percentage of intact (Int), swollen (Swo) and reacted (Rea) sperm. Data were compared using the chi-square test for two sets of data. ***$P <$ 0.001. Plotted are average ± range of two independent experiments.

microscope at 50 kV. We included negative (not stimulated) and positive (stimulated with A23187 or progesterone in the presence of 20 μM BAPTA-AM to inhibit the final stages of the AR without affecting acrosomal swelling) controls in all experiments. At least 100 cells were counted per condition and acrosomal patterns were classified as intact, reacted (vesiculated and lost), and swollen (enlarged and deformed).

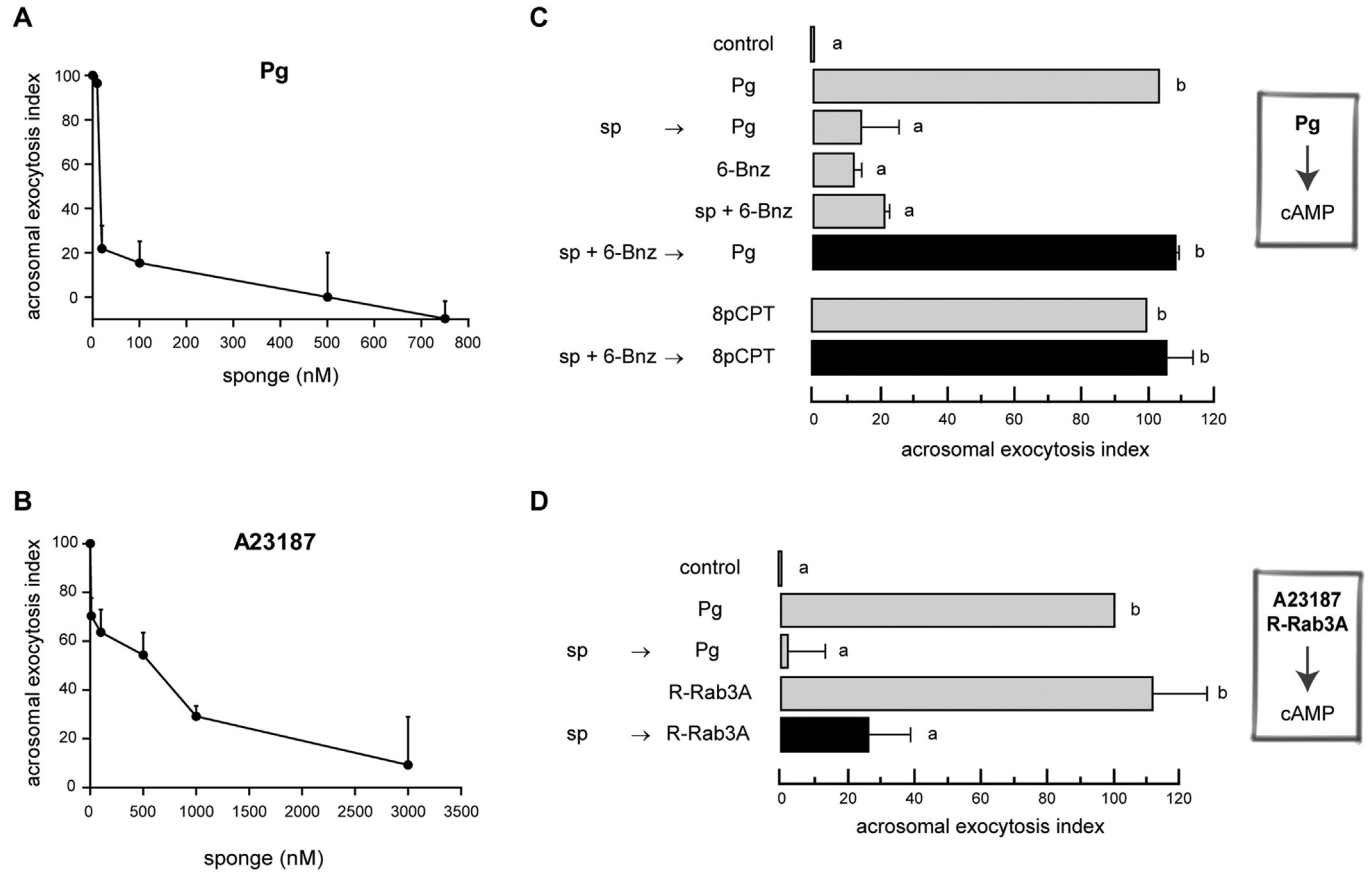

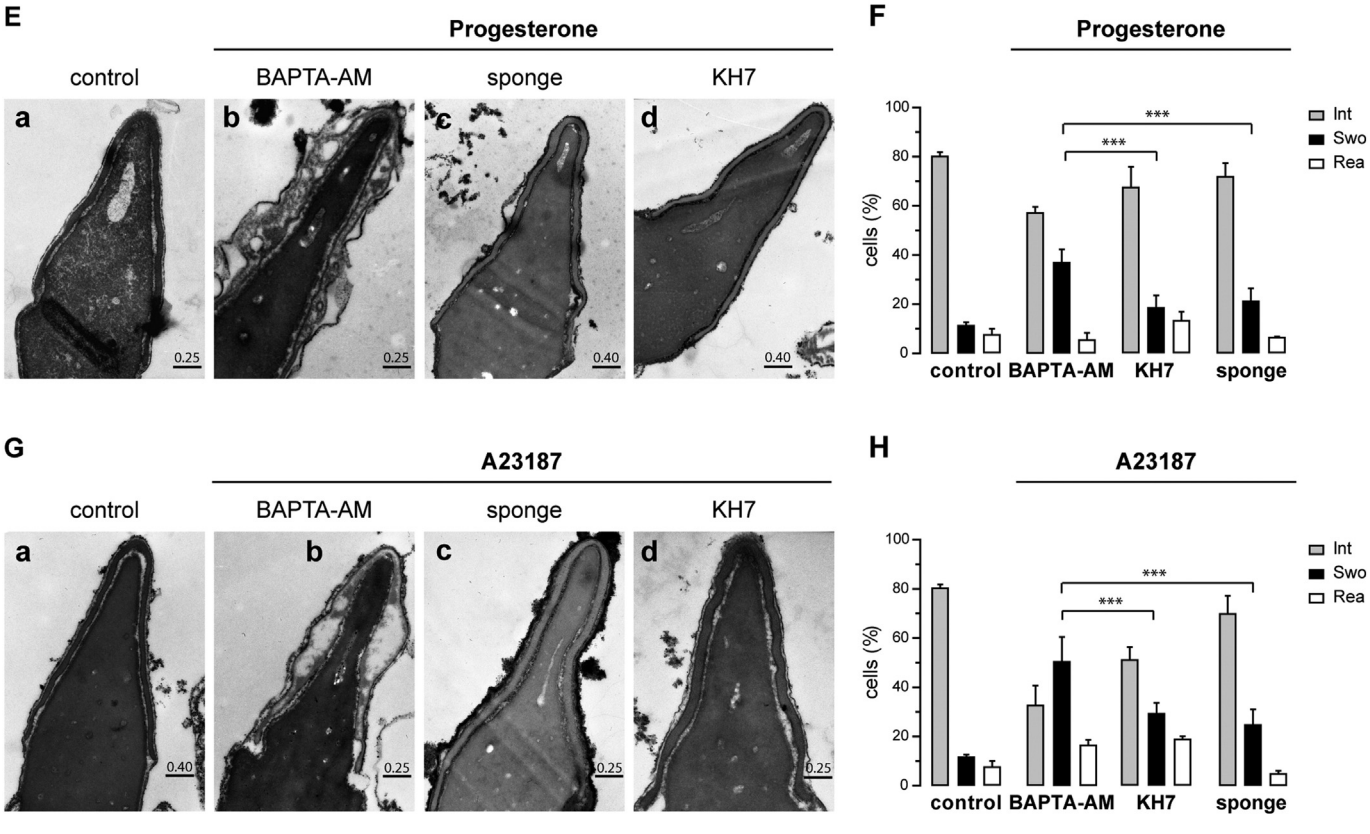

Data were plotted and analyzed with the program GraphPad Prism 5 using the chi-square test for pairwise comparisons. Differences were considered significant at the $P < 0.05$ level

3. Results

3.1. The TAT-cAMP sponge transduces into human sperm

The biggest stumbling block when trying to apply classic cell biology and biochemistry approaches to sperm resides on their inability to synthesize proteins. Our laboratory has successfully contributed to establishing two techniques to overcome this limitation: controlled plasma membrane permeabilization with pore-forming toxins and delivery of permeable proteins. The latter allows sophisticated molecular studies of the pathways elicited by well-established AR inducers because it grants access to intracellular compartments in non-permeabilized cells. Here, we describe a tool designed to unveil cAMP-related signaling pathways and their regulation in live sperm, something difficult to achieve, save for pharmacological and genetic approaches. We designed a permeable version of the cAMP sponge [33] that possesses the sequence of the C-terminal domain of human PKA-RIβ (aa 132–381) coupled to the protein transduction domain TAT of human immunodeficiency virus-1 [27] and a His_6-tag for purification and detection (Fig. 1A). We analyzed the incorporation – confirmed by resistance to tryptic digestion – of the TAT-cAMP sponge into human sperm by Western blot and indirect immunofluorescence with anti-His_6 antibodies. First, we conducted dose–response experiments to determine the minimal amount of trypsin required to digest 1 μM TAT-cAMP sponge. The minimal amount of trypsin capable of erasing the anti-His_6 signal was 1 μg/ml, with 0.5 μg/ml causing partial and 0.1 μg/ml very little cleavage (Fig. 1B). Degradation products were visible in Coomassie blue-stained gels (data not shown) but not by Western blot because of the many trypsin cleavage sites present in the sequence of the protein (assessed by ExPASy Peptide Cutter), one is very near the His_6 tag. Thus, when trypsin cuts the sponge at this site, fragments are not visible with the anti-His_6 antibodies. Next, we incubated sperm with the TAT-cAMP sponge for 15 min, divided the sample, and added 0.1 μg/ml trypsin (negative control) to one tube and 1 μg/ml to the other. After incubation, we recovered both the cells and the supernantant and processed them for anti-His_6 Western blot. A significant proportion of the TAT-cAMP sponge was internalized by human sperm and not merely adhered to the extracellular face of the plasma membrane because the signal was resistant to tryptic digestion (Fig. 1C, "incorporated"). Trypsin (1 μg/ml) removed the His_6 signal of all the TAT-cAMP sponge remaining in the supernatant, indicating that the enzyme was active and its concentration sufficient (Fig. 1C, "unincorporated"). We conducted similar experiments, revealing the transduction of the TAT-cAMP sponge by indirect immunofluorescence. A high number (86%) of cells exhibited trypsin-resistant staining mainly in the acrosomal region and mid piece or entire flagellum (Fig. 1D). Neither cells treated with the TAT-cAMP sponge but without primary antibodies nor those treated with the antibodies but without the sponge showed any detectable signal, suggesting that the staining was specific. These experiments show that the TAT-cAMP sponge transduced into human sperm.

3.2. Progesterone, R-Rab3A, and the calcium ionophore A23187 require cAMP to accomplish acrosomal content release

We started by testing the effect of the TAT-cAMP sponge on the AR triggered by two widely used inducers: progesterone and A23187. The sponge inhibited these exocytosis in a dose–response manner. TAT-cAMP sponge (100 nM) inhibited the AR triggered by progesterone by ≈80% (Fig. 2A), whereas a higher concentration was necessary to prevent that elicited by A23187 (Fig. 2B). This might be due to a larger accumulation of cAMP in sperm as a consequence of the more robust calcium influx evoked by the ionophore. To test the specificity of the TAT-cAMP sponge, we preincubated it with 6-Bnz-cAMP, an analog known to bind PKA's cAMP-binding sites, before introducing it into sperm. Because the sponge contains two cAMP-binding sites, we used 200 nM 6-Bnz-cAMP to saturate 100 nM TAT-cAMP sponge. Progesterone and 8-pCPT-2′-*O*-Me-cAMP accomplished the AR normally in sperm loaded with the TAT-cAMP sponge preincubated with 6-Bnz-cAMP (Fig. 2C, black bars). These results indicate that the ability of the TAT-cAMP sponge to inhibit the AR was due to its capacity to sequester endogenous cAMP. In other words, the TAT-cAMP sponge is a reliable, specific tool to monitor cAMP-driven pathways. A permeant version of recombinant Rab3A (R-Rab3A), when geranylgeranylated and persistently active, induces the AR in non-permeabilized sperm as does the non-permeant version in SLO-treated sperm [34]. To ask whether this AR inducer also needs cAMP to achieve exocytosis, we depleted sperm of cAMP with the TAT-cAMP sponge before challenging with permeable Rab3A. The AR was inhibited under these conditions (Fig. 2D, black bar). These results suggest that, similarly to progesterone, R-Rab3A relies on endogenous cAMP to achieve exocytosis.

Osmotic swelling of secretory granules and vesicles is proposed to be an intermediate step in the exocytic fusion of the granules with the plasma membrane [20]. Sperm are not the exception to this rule [69]. Swollen acrosomes are seldom observed by transmission electron microscopy in resting sperm but can be transiently detected in sperm that have initiated exocytosis before they lose their acrosomes completely. To halt the AR and capture cells with swollen acrosomes, we incubated sperm with 20 μM BAPTA-AM. This high affinity, fast calcium chelator permeates through the plasma membrane into the cytosol. At 20 μM, enough BAPTA-AM crosses the acrosomal membrane to reach the acrosome [57]. BAPTA-AM halts the exocytotic cascade at a post-swelling stage because it allows the reaction to proceed all the way until intra-acrosomal calcium release is required [34,46]. The percentage of resting sperm with swollen acrosomes was very low. This percentage increased to ≈40% upon treatment with BAPTA-AM and progesterone. Preincubation with the TAT-cAMP sponge prevented progesterone from inducing acrosomal swelling, which was only observed in ≈20% cells (Fig. 2F). Likewise, challenging with A23187 in the presence of BAPTA-AM caused swelling in ≈50% cells; this percentage was reduced to ≈25% by the TAT-cAMP sponge (Fig. 2H). These data provide direct evidence that progesterone and A23187 require cAMP to induce acrosomal swelling, an essential intermediate stage during sperm exocytosis.

To gain further insight into the mechanism through which sperm require cAMP to accomplish acrosomal swelling, we prevented its synthesis with the soluble adenylyl cylase (sAC) blocker KH7. Neither progesterone (Fig. 2Ed) nor A23187 (Fig. 2Gd) were able to swell acrosomes when sperm were pretreated with KH7. These data suggest that AR inducers

Fig. 3. Progesterone activates Rap1, Rab3, and Rab27 in the acrosomal region in a cAMP-dependent manner. Capacitated human sperm were incubated with 100 μM 2-APB and, when indicated, with 100 nM TAT-cAMP sponge (sp, B–D) or 10 μM H89 (E), followed by 10 μM A23187 (A) or 15 μM progesterone (Pg, A–E), 50 μM 8-pCPT-2′-*O*-Me-cAMP (8-pCPT) or 200 μM 6-Bnz-AMPc (6-Bnz) (E) for 15 min at 37 °C. Cells were processed for far-immunofluorescence as described in Section 2.9, overlain with GST-Ral-GDS-RBD to detect active Rap1 (A, B, E), GST-Slac2-b-SHD to detect active Rab27 (C) or GST-RIM-RBD to detect active Rab3 (D) and triple stained with the anti-GST antibody (to visualize the activity probes; red, left panels), FITC-PSA (to confirm that the AR was effectively prevented by 2-APB; green, central panels), and Hoechst 33342 (to visualize all cells in each field; blue, right panels). Shown are epifluorescence micrographs of typically stained cells. Bars = 5 μm. (A–D) Quantifications of the percentage of cells with active GTPases in the acrosomal region are shown at the bottom of each group of micrographs. Tukey–Kramer post hoc test was used for pairwise comparisons. The data represent the mean ± SEM of three independent experiments. $^{*}P < 0.05$; $^{**}P < 0.01$; $^{***}P < 0.001$. (E) The percentage of cells with acrosomal Rap1 in the control condition (untreated cells) was subtracted from all values. Different letters indicate statistical significance ($P < 0.001$).

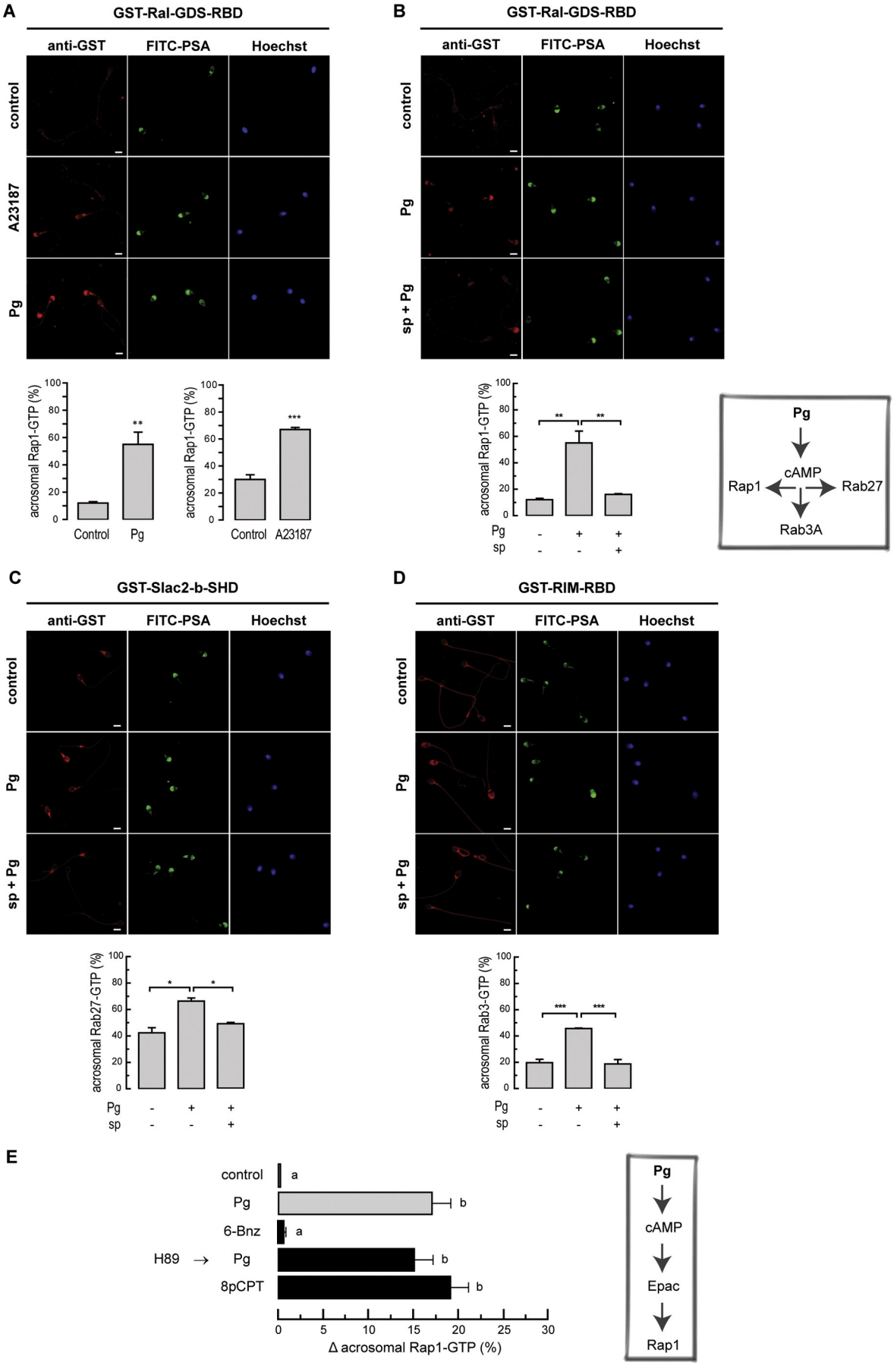
A
GST-Ral-GDS-RBD
anti-GST
FITC-PSA
Hoechst
control
A23187
Pg
acrosomal Rap1-GTP (%)
Control
Pg
Control
A23187
B
GST-Ral-GDS-RBD
sp + Pg
Pg
sp
Pg
cAMP
Rap1
Rab27
Rab3A
C
GST-Slac2-b-SHD
acrosomal Rab27-GTP (%)
D
GST-RIM-RBD
acrosomal Rab3-GTP (%)
E
6-Bnz
H89
8pCPT
Δ acrosomal Rap1-GTP (%)
Epac

require cAMP synthesized by sAC to achieve acrosomal swelling. The morphologies scored in the quantifications (Fig. 2F and H) are "intact" (Int), meaning unswollen acrosomes and illustrated in micrographs a, c, and d of both series; "swollen" (Swo), meaning swollen acrosomes and illustrated in micrographs b of both series; and "reacted" (Rea), meaning lost acrosomes and not shown in the micrographs (but see [69]).

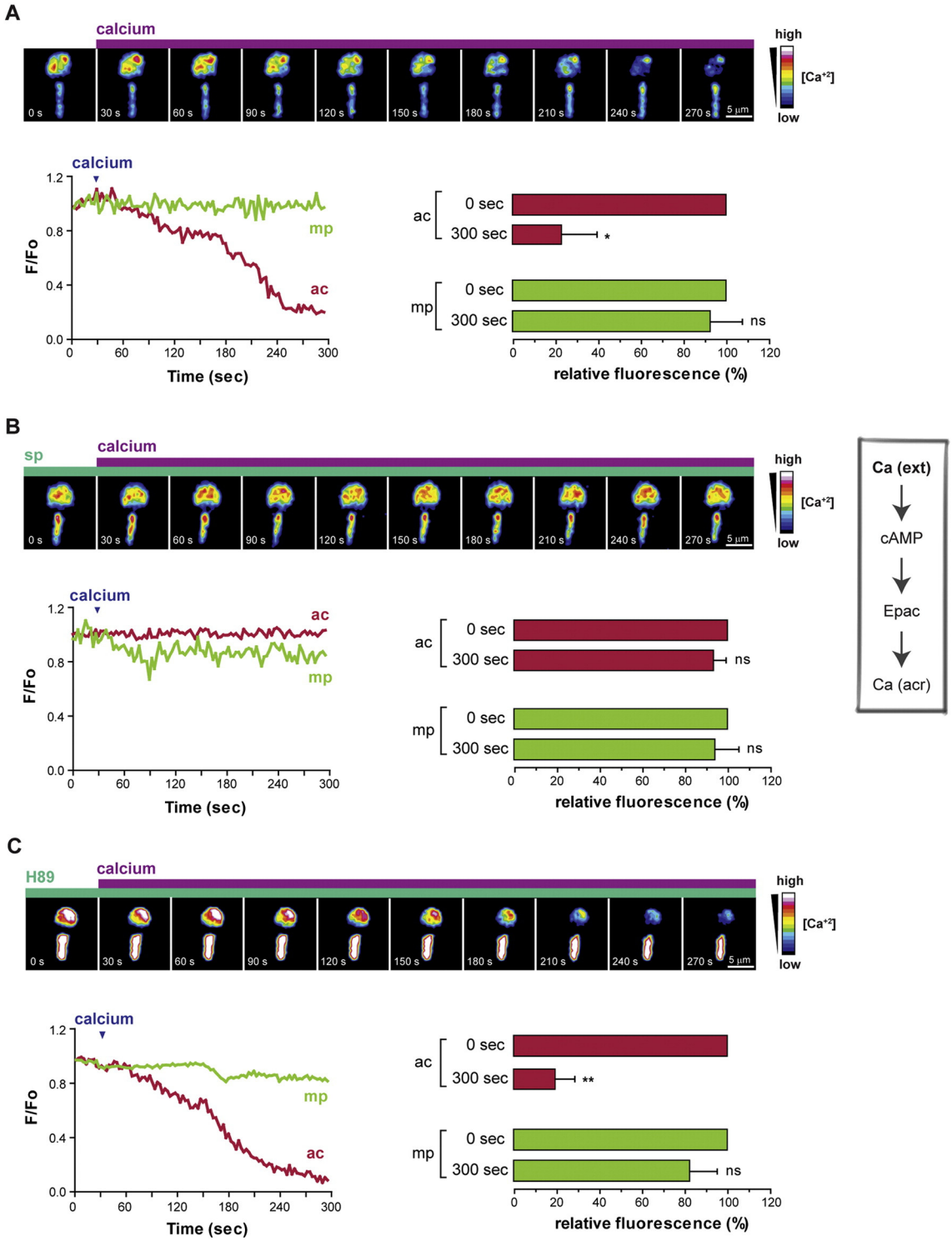

Fig. 4. Extracellular calcium elicits calcium release from the acrosomal store in a cAMP/Epac-dependent and PKA-independent manner. Capacitated, SLO-permeabilized human sperm were treated with 100 nM botulinum toxin B to prevent exocytosis, loaded with the fluorescent calcium indicator Fluo3-AM (2 μM) and incubated with 100 nM TAT-cAMP sponge (B, sp) or 10 μM H89 (C). Samples were stimulated with 0.5 mM $CaCl_2$ (calcium) and the fluorescence intensity visualized as described in Section 2.10. Images are pseudo-colored to show intensity of fluorescence. Scales are shown on the right ("warm" colors represent high $[Ca^{2+}]$). Numbers below the images indicate time in seconds. Changes in fluorescence were localized to the acrosome; fluorescence in the mid piece was invariant. Scale bars = 5 μm. Each line graph shows the recording of $[Ca^{2+}]$ changes in the same cell shown above. Plotted are the normalized Fluo3 fluorescence variations in the acrosome (ac, red) and the mid piece (mp, green) in response to the application of $CaCl_2$ (indicated by vertical arrows) vs. time. Bar graphs illustrate the population response to each treatment (mean ± SEM; 6–13 cells in three experiments). Shown is the relative fluorescence from the acrosomal (ac, red) and mid piece (mp, green) regions at the beginning (0 s, assigned 100%) and 300 s after the initiation of the recording. Asterisks indicate significant difference ($^*P < 0.05$; $^{**}P < 0.01$) from the initial value (single group analysis, 95% confidence interval); ns indicates that statistical difference from the initial value was nonsignificant ($P > 0.05$).

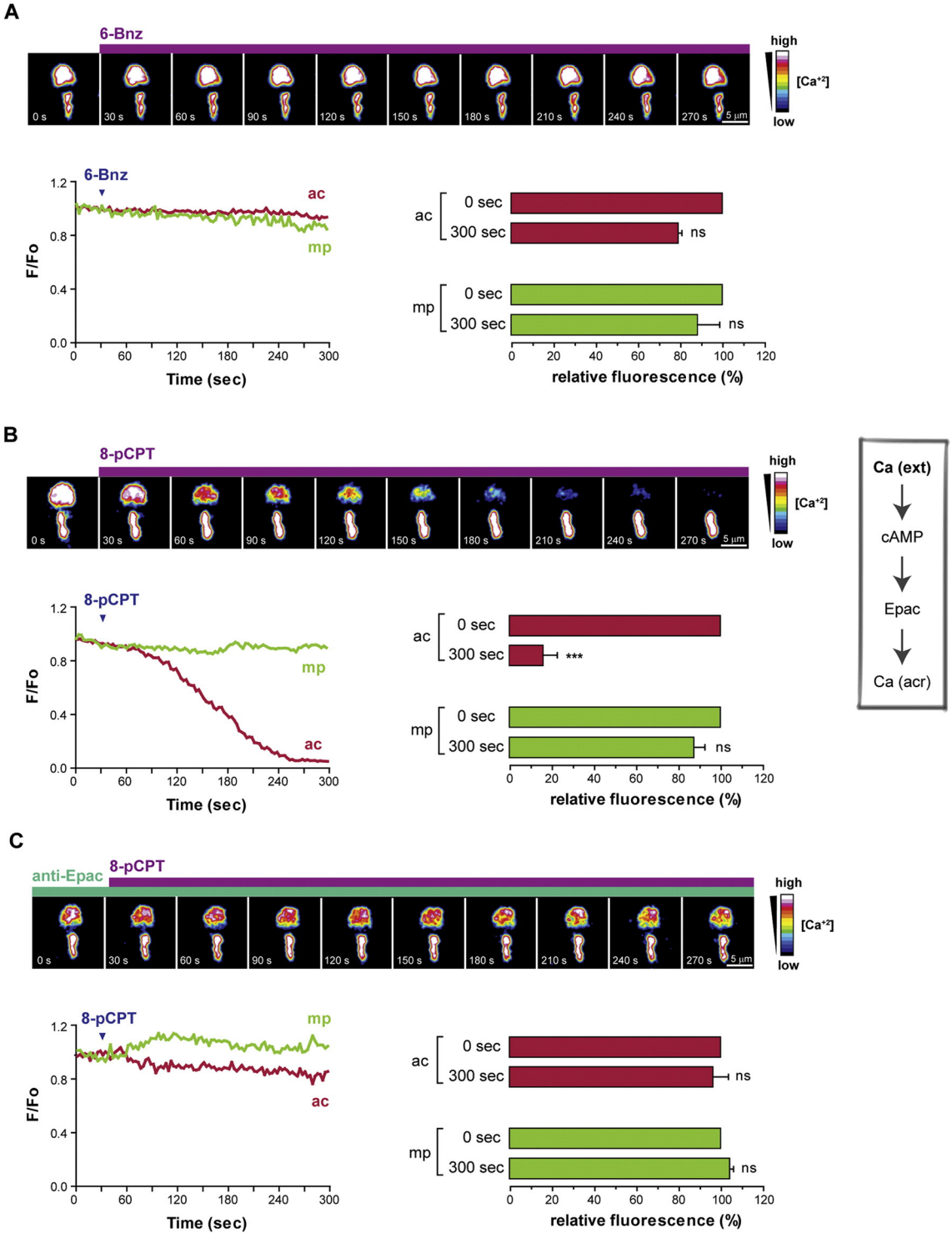

Fig. 5. Epac stimulation elicits calcium release from the acrosomal store. Experiments were conducted and data analyzed and plotted as described in the legend to Fig. 4 except that 0.5 mM $CaCl_2$ was replaced by 200 µM 6-Bnz-AMPc (6-Bnz, A) or 50 µM 8-pCPT-2′-*O*-Me-cAMP (8-pCPT, B, C). C, cells were treated with 6.7 nM anti-Epac antibodies for 15 min at 37 °C before the cAMP analog. Bar graphs illustrate the population response to each treatment (mean ± SEM; 7–17 cells in three experiments). Asterisks indicate significant difference (***$P < 0.001$) from the initial value (single group analysis, 95% confidence interval); ns indicates that statistical difference from the initial value was nonsignificant ($P > 0.05$).

3.3. Progesterone, R-Rab3A, and the calcium ionophore A23187 activate Rap1 during the exocytotic cascade

Based on data gathered with SLO-permeabilized cells, we have put together a model for some of the biochemical events during the AR in human sperm where we propose that they are organized in a bifurcated pathway. cAMP/Epac sit at a central point of the signaling cascade after which the exocytotic pathway splits into two limbs that must act in concert to achieve exocytosis. Each limb is headed by a small GTPase: the limb that culminates on the productive assembly of the fusion machinery begins with the activation of Rab3; the limb that elicits the release of intracellular calcium starts with the activation of Rap1 [8,47]. Rab27, another secretory Rab, acts upstream of Rab3 [11]. We have developed a far-immunofluorescence technique that allows

simultaneous determination of the activation status and localization of Rabs 3 and 27 [11] and Rap1 [47] in individual cells. Briefly, the method consists of overlaying sperm fixed on slides with protein cassettes corresponding to active small GTPase-binding domains from known effectors, fused to GST. These activity probes are subsequently detected by indirect immunofluorescence with anti-GST antibodies. A similar approach has been described to assess the activation status of Ras2 in *Saccharomyces cerevisiae* [23]. By means of this technology, we have shown that Rap1 exchanges GDP for GTP in response to the initiation of the AR with external calcium in SLO-permeabilized human sperm [47]. Rap1 is the Rap isoform predominantly pulled down by Ral-GDS-RBD [21]. Only Rap1 has been described in human sperm [8]. In addition, the acrosomal Rap-GTP signal is erased by preincubation with anti-Rap1 antibodies [47]. Thus, we conclude that Rap1 is likely the isoform detected by Ral-GDS-RBD in human sperm and therefore we will refer to active Rap1 throughout this manuscript.

We conducted far-immunofluorescence assays to ask whether Rap1 is activated in response to AR inducers in non-permeabilized sperm. Ral-GDS-RBD detected active Rap1 in the acrosomal region of a small population of resting cells. The percentage increased significantly upon incubation with progesterone or A23187 (Fig. 3A). Likewise, permeable, geranylgeranylated and active Rab3A increased in 25 ± 3.65% above the control the number of cells with acrosomal Rap1-GTP (Fig. S1, top black bar). The activation of Rap1 in the acrosomal region was comparable to that achieved by progesterone (22.25 ± 2.66% above the control, gray bar). Taken together, these results suggest that the activation of Rap1 is an essential step in the exocytosis cascade triggered by all AR inducers.

3.4. Progesterone promotes the activation of Rap1, Rab3, and Rab27 via cAMP-dependent pathways

Because of its relevance as physiological AR trigger, we focused on progesterone to conduct the experiments we will describe next. To determine whether this inducer requires cAMP to activate Rap1, we carried out far-immunofluorescence experiments similar to the ones described above but depleting sperm from cAMP by preincubation with the TAT-cAMP sponge. Ral-GDS-RBD detected active Rap1 in 12% of resting cells. The percentage increased to 55% upon treatment with progesterone. The sponge prevented progesterone from activating Rap1 (Fig. 3B). Preincubation with the TAT-sponge also inhibited the activation of Rap1 by R-Rab3A (Fig. S1, bottom black bar). These results suggest that the mechanism involved in Rap1 activation elicited by the two AR inducers requires cAMP.

Next, we asked whether progesterone activates Rabs3 and 27 to accomplish the AR. We replaced Ral-GDS-RBD by a Slac2-b-SHD cassette that binds Rab27-GTP and found that this was the case (Fig. 3C). Likewise, far-immunofluorescence experiments using RIM-RBD as activity probe showed that Rab3 was activated in the acrosomal region in response to progesterone (Fig. 3D). In both cases, preincubation with the TAT-cAMP sponge abolished the stimulatory effect of progesterone on the activation of secretory Rabs. Taken together, our data indicate that the signaling cascade initiated by progesterone activates all three small G proteins and that it does so via a cAMP-mediated mechanism. The importance of these findings is twofold: first, they contribute to the biochemical characterization of the exocytotic cascade triggered by progesterone during the AR. Second, they point to the robustness and reliability of the SLO-permeabilized sperm model to elucidate the signal transduction pathways that drive the AR.

3.5. Progesterone activates Rap1 via an Epac-dependent and PKA-independent pathway

Because the activation of sperm Rap1 by progesterone was mediated by cAMP, we investigated which was the target involved. The treatment of human sperm with the PKA-selective analog 6-Bnz-cAMP did not result in the activation of endogenous Rap1. Furthermore, progesterone continued to augment the percentage of cells with Rap1-GTP in the acrosomal region even after pretreatment with H89, an isoquinoline sulfonamide that selectively inhibits PKA (Fig. 3E). These results suggest that the cAMP-dependent increase in Rap1-GTP elicited by progesterone was not due to the activation of PKA. We measured a strong activation of Rap1 within 15 min of exposure to the Epac-selective analog 8-pCPT-2′-*O*-Me-cAMP (Fig. 3E). These data demonstrate that the activation of sperm Epac leads to the exchange of GDP for GTP on endogenous Rap1. Despite the fact that the AR elicited by progesterone in human sperm is sensitive to H89 [9], it would appear that the pathway involving PKA does not include the activation of Rap1.

3.6. Acrosomal calcium is mobilized by a cAMP/Epac-dependent and PKA-independent pathway

Our next goal at this point was to fill in the gaps between cAMP and intra-acrosomal calcium mobilization in the AR signaling pathway. This is better achieved in the SLO-permeabilized sperm model because it is more versatile than live preparations. Simply bathing permeabilized sperm suspended in an isotonic buffer with 0.5 mM $CaCl_2$ elicits exocytosis. Preincubation with the TAT-cAMP sponge inhibited calcium-triggered exocytosis in a dose–response fashion, reaching maximum inhibition at 100 nM (Fig. S2A). Therefore, we selected this concentration of the TAT-cAMP sponge for the remaining experiments.

Sequestering endogenous cAMP should halt the AR at a step prior to intra-acrosomal mobilization. We tested this prediction with the photosensitive calcium chelator NP-EGTA-AM. In the SLO-permeabilized human sperm model, this reagent crosses the plasma and outer acrosomal membranes, accumulates inside the acrosome, and prevents the AR triggered by all inducers by sequestering intra-acrosomal calcium for as long as the system is kept in the dark. UV photolysis of NP-EGTA-AM rapidly replenishes the acrosomal calcium pool, resuming exocytosis [1,16,25]. In NP-EGTA-AM-loaded permeabilized sperm, the TAT-cAMP sponge blocked exocytosis when added before, but not after, initiating the AR with calcium (Fig. S2B). These data confirm that cAMP plays its role in exocytosis prior to intra-acrosomal calcium efflux. In the next section, we investigated if and how does cAMP drive intra-acrosomal calcium mobilization.

Fluo3-AM is an intracellular calcium indicator that is practically non-fluorescent in its ligand-free form. When sperm with their plasma membrane permeabilized with SLO are exposed to Fluo3-AM, the dye

Fig. 6. PLCε is required for the AR downstream of Rap1 and upstream of intra-acrosomal calcium mobilization. (A) Human sperm were immunostained with (top) or without (bottom) antibodies to PLCε as described in Section 2.8 (see legend to Fig. 1D). (B) Permeabilized human sperm were treated for 15 min at 37 °C with increasing concentrations of anti-PLCε antibodies. The AR was initiated with 0.5 mM $CaCl_2$, incubating as before. (C) Sperm were incubated with 6.7 nM anti-PLCε antibodies for 15 min at 37 °C and subsequently challenged with 50 μM 8-pCPT-2′-*O*-Me-cAMP (8-pCPT) (top black bar). Alternatively, spermatozoa were treated with 6.7 nM anti-PLCε antibodies, 0.5 mM $CaCl_2$ and 5 μM adenophostin A (AdA) incubating 10 min at 37 °C after each addition (bottom black bar). (D, E) Sperm were loaded with 134 nM anti-Rap1 antibodies, 0.5 mM $CaCl_2$, 15 μM U73122 (D), or 6.7 nM anti-PLCε antibodies (E) and 453 μg/ml (283 nM) Rap1 peptide (black bars). Samples were incubated for 8 min at 37 °C after each addition. (F) Spermatozoa were loaded with 10 μM NP-EGTA-AM (NP) for 10 min at 37 °C. The AR was initiated with 0.5 mM $CaCl_2$ followed by 6.7 nM anti-PLCε antibodies with 15 min at 37 °C incubations. All procedures were carried out in the dark. Last, UV photolysis of the chelator was induced (hν, black bar). (B–F) The AR was measured as described in Section 2.7. The data represent the mean ± SEM of at least three independent experiments. Controls (gray bars) include background AR (control) in the absence of any stimulation; AR stimulated by 0.5 mM $CaCl_2$ (calcium) or 50 μM 8-pCPT-2′-*O*-Me-cAMP (8-pCPT), inhibition by 134 nM anti-Rap1, 6.7 nM anti-PLCε antibodies, 15 μM U73122, or NP-EGTA-AM in the dark, and the inhibitory effect of the blockers when present throughout the experiments; rescue of the anti-Rap1 antibodies by the Rap1 peptide and recovery of the AR in sperm loaded with NP-EGTA-AM on illumination. Different letters indicate statistical significance (C–E, $P < 0.001$; F, $P < 0.5$).

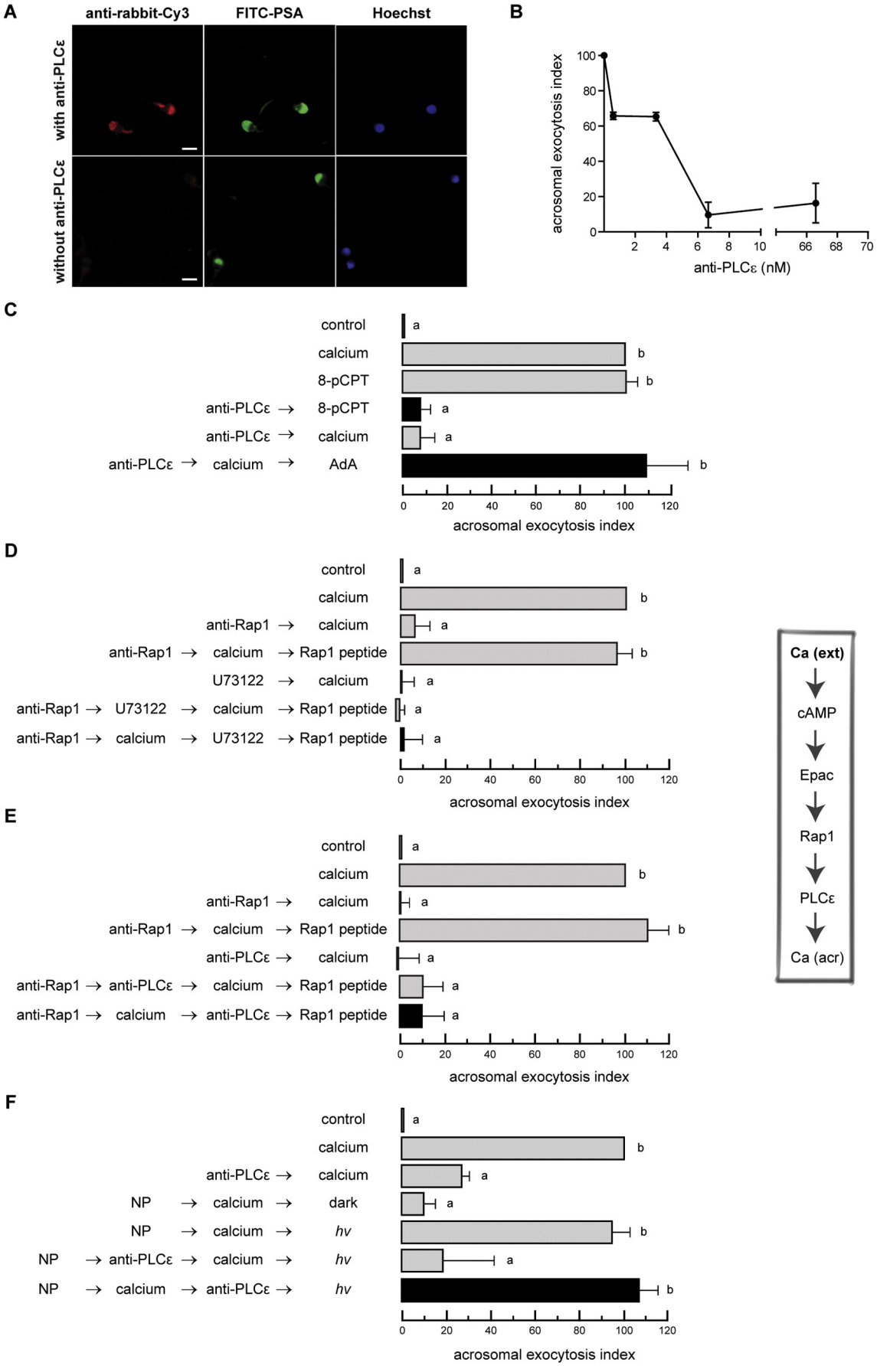
A
anti-rabbit-Cy3
FITC-PSA
Hoechst
with anti-PLCε
without anti-PLCε
B
acrosomal exocytosis index
anti-PLCε (nM)
C
control
calcium
8-pCPT
anti-PLCε → 8-pCPT
anti-PLCε → calcium
anti-PLCε → calcium → AdA
acrosomal exocytosis index
D
control
calcium
anti-Rap1 → calcium
anti-Rap1 → calcium → Rap1 peptide
U73122 → calcium
anti-Rap1 → U73122 → calcium → Rap1 peptide
anti-Rap1 → calcium → U73122 → Rap1 peptide
acrosomal exocytosis index
E
control
calcium
anti-Rap1 → calcium
anti-Rap1 → calcium → Rap1 peptide
anti-PLCε → calcium
anti-Rap1 → anti-PLCε → calcium → Rap1 peptide
anti-Rap1 → calcium → anti-PLCε → Rap1 peptide
acrosomal exocytosis index
F
control
calcium
anti-PLCε → calcium
NP → calcium → dark
NP → calcium → hv
NP → anti-PLCε → calcium → hv
NP → calcium → anti-PLCε → hv
acrosomal exocytosis index
Ca (ext)
cAMP
Epac
Rap1
PLCε
Ca (acr)

diffuses into the acrosome and the mitochondria in the mid piece, where esterases remove the AM moiety and thus trap the sensor. Once inside these organelles, Fluo3 becomes fluorescent upon binding to calcium. Thanks to the SLO permeabilization protocol, we can actually visualize the human sperm acrosomal calcium store with Fluo3-AM (Figs. 4, 5, 7, S3 and [16,35,41,47]). This is more difficult to achieve in non-permeabilized sperm, where cytosolic esterases remove the AM moiety, trapping membrane impermeant Fluo3 in the cytosol. The concentration of calcium in the granule remained high and without appreciable changes in concentration during 5 min incubation at 37 °C (data not shown but see [47]). Extracellular calcium, the AR inducer used in the experiments shown in Fig. S2, depleted the acrosomal calcium store in 3–5 min (Fig. 4A). To avoid confusion in the read out between calcium signal loss (due to efflux from the acrosome) and acrosomal loss (due to exocytosis), we performed these measurements in the presence of botulinum toxin B, a late AR blocker. The mid piece harbors the sperm mitochondria; as expected, calcium from this reservoir was not mobilized in response to the onset of exocytosis (Figs. 4, 5, 7 and S3, mp, green lines/bars). When cAMP was sequestered by the TAT-cAMP sponge, external calcium failed to induce vesicular calcium efflux (Fig. 4B). Who is the target cAMP binds to? It does not appear to be PKA, because inhibiting its catalytic activity with H89 did not interfere with external calcium-triggered intra-acrosomal calcium mobilization (Fig. 4C), nor did treatment with the PKA-selective analog 6-Bnz-cAMP mobilize calcium (Fig. 5A). In contrast, incubation with the Epac-selective analog 8-pCPT-2′-*O*-Me-cAMP readily evoked internal calcium mobilization (Fig. 5B). These results indicate that cAMP provokes intra-acrosomal calcium mobilization via the activation of its target Epac. Last, we preincubated the cells with anti-Epac antibodies before challenging with 8-pCPT-2′-*O*-Me-cAMP; under these conditions, the analog failed to mobilize calcium (Fig. 5C). In short, our results provide direct evidence that cAMP and its target Epac are essential components of the signaling pathway that mobilizes intra-acrosomal calcium to achieve exocytosis.

3.7. A PLCε is required for the AR downstream of Rap1 and upstream of intra-acrosomal calcium mobilization

What are the missing components of the signaling pathway that joins cAMP/Epac with intracellular calcium mobilization? Rap1-GDP serves as a substrate for cAMP/Epac and therefore Rap1-GTP is likely to be one such component. What would its target be? Calcium is mobilized from the acrosome through IP_3-sensitive channels [16,47]. Therefore, our first candidate was PLCε, because it is both a Rap effector and one of the enzymes that hydrolyzes PIP_2 to generate IP_3. PLCε has been detected in a mouse testis transcriptome enriched in germ cells [52] and in mouse type A spermatogonia, pachytene spermatocytes, and round spermatids RNAs [66]. In addition, a probe detected PLCε on a chip that contains mRNAs from human germ cells (http://biogps.org/dataset/GSE1133/). We investigated the presence of this enzyme in human sperm by indirect immunofluorescence and found it to localize, although not exclusively, to the acrosomal region (Fig. 6A, top, red). This is the subcellular localization expected of a protein with a role in the AR. Next, we introduced anti-PLCε antibodies into SLO-permeabilized human sperm and monitored their effect on the calcium-triggered AR. Sequestration of sperm PLCε by specific antibodies inhibited calcium-triggered exocytosis in a dose–response fashion, reaching maximum inhibition at 6.7 nM (Fig. 6B). Therefore, the remaining experiments were conducted with this concentration. The AR elicited by 8-pCPT-2′-*O*-Me-cAMP was also sensitive to 6.7 nM anti-PLCε antibodies (Fig. 6C, top black bar). The anti-PLCε antibodies we selected for this study are raised against a peptide located in the RA2 domain of the protein, which is not present in other PLC isoforms [56]. Thus, the chances that the inhibitory effect of the anti-PLCε antibodies might be due to cross-reactivity with other PLCs are low. Nevertheless, we carried out experiments identical to those summarized in Fig. 6B and C but substituting the anti-PLCε by anti-PLCγ1 antibodies in an effort to confirm the specificity of the effect of the former. We selected anti-PLCγ1 antibodies raised against a peptide not present in PLCε. These antibodies did not inhibit the AR triggered by calcium or 8-pCPT-2′-*O*-Me-cAMP (Fig. S3A-B). In short, our data indicate that PLCε is necessary for the human sperm AR.

We hypothesized that signaling through PLCε, with the ensuing production of IP_3, drives the intracellular calcium mobilization required for the AR. If this was the case, then anti-PLCε antibodies blocked exocytosis because they prevented calcium mobilization. We tested this possibility with an indirect (AR assay, Fig. 6C and F) and a direct (calcium mobilization, Fig. 7D) approaches. In AR assays, the IP_3 receptor agonist adenophostin A (AdA) promotes intravesicular calcium release and rescues the blockage on calcium-triggered exocytosis imposed by anti-Rap1 antibodies [8,47]. The sole addition of adenophostin A rescued exocytosis impaired by anti-PLCε antibodies (Fig. 6C, bottom black bar), supporting the notion that the end point of the PLCε-catalyzed step is the mobilization of intracellular calcium.

To narrow down the step in the cascade where PLCε is required, we exploited a remarkable feature of the permeabilized sperm model that confers the ability of reversibly halting exocytosis at specific stages (see [8,11,47] for examples of reversible pairs previously used to study stage-specific components of the AR). In this case, we used anti-Rap1 antibodies, known to block the AR in SLO-permeabilized human sperm [8,35,47], as the inhibitor component and the peptide against which the antibodies were raised as the rescue component of the reversible pair. Anti-Rap1 antibodies preincubated with this peptide are unable to block the AR [8]. Here we show that the Rap1 peptide was able to rescue the inhibitory effect of the antibodies when added to permeabilized sperm at the end of the incubation, demonstrating that the anti-Rap1/Rap1 peptide behaves as a suitable reversible pair (Fig. 6D, E). The mechanism is as follows: the antibodies sequester endogenous Rap1 and impair its actions, halting the AR at the stage when Rap1 is required; Rap1 peptide added at the end of the incubation displaces the antibody from sperm Rap1 and allows the exocytotic cascade to resume.

If the target of the inhibitor to test is required before Rap1, the reaction will not be inhibited by adding it after anti-Rap1 and calcium (sequence of additions: anti-Rap1 → calcium → inhibitor to test → Rap1 peptide). On the contrary, if the target is required after the AR has progressed up to the step when Rap1 is required, the inhibitor will arrest the reaction in a manner that the Rap1 peptide will not be able to overcome. To ask whether a PLC activity is required after Rap1, we tested the effect of U73122, an inhibitor of multiple phosphatidylinositol-specific PLC isoforms, in the context of the anti-Rap1/Rap1 peptide reversible pair. The AR was inhibited (Fig. 6D, black bar), which suggests that a PLC is necessary downstream of Rap1. Next, we conducted similar experiments but replacing U73122 by anti-PLCε antibodies. Once again, the Rap1 peptide was unable to overcome the exocytotic block (Fig. 6E, black bar). These results indicate that PLCε exhibits its role in the AR downstream that of Rap1.

AR inducers trigger a cascade that activates PLCε through the pathway cAMP/Epac/Rap1/PLCε. The results shown in Fig. 6C (anti-PLCε → calcium → AdA) suggest that the site of the cascade where PLCε exhibits

Fig. 7. 8-pCPT-2′-*O*-Me-cAMP requires Rap1 and PLCε to mobilize calcium from the acrosomal store. (A) Experiments were conducted and data analyzed and plotted as described in the legend to Fig. 4 except that 0.5 mM $CaCl_2$ was replaced by 50 μM 8-pCPT-2′-*O*-Me-cAMP (8-pCPT). SLO-permeabilized cells were treated with 134 nM anti-Rap1 antibodies (B), 15 μM U73122 (C), or 6.7 nM anti-PLCε antibodies (D) for 15 min at 37 °C before adding the cAMP analog. Bar graphs illustrate the population response to each treatment (mean ± SEM; 5–15 cells in three experiments). Asterisks indicate significant difference (***$P < 0.001$) from the initial value (single group analysis, 95% confidence interval), ns indicates that statistical difference from the initial value was nonsignificant ($P > 0.05$).

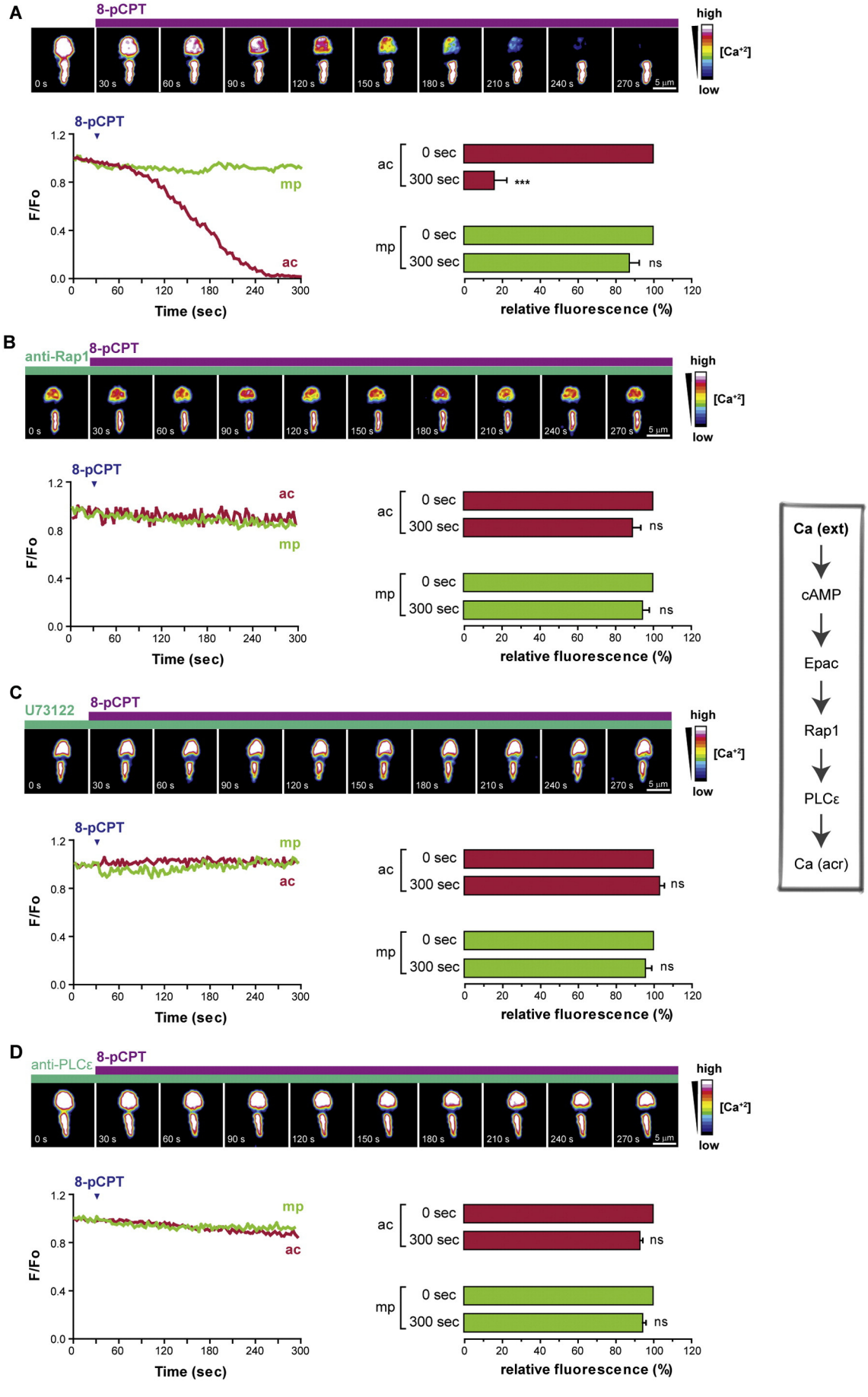
A
8-pCPT
high
[Ca+2]
low
0 s
30 s
60 s
90 s
120 s
150 s
180 s
210 s
240 s
270 s
5 µm
8-pCPT
F/Fo
mp
ac
Time (sec)
ac
0 sec
300 sec
***
mp
0 sec
300 sec
ns
relative fluorescence (%)
B
anti-Rap1
8-pCPT
C
U73122
8-pCPT
D
anti-PLCε
8-pCPT
Ca (ext)
cAMP
Epac
Rap1
PLCε
Ca (acr)

its role is upstream intra-acrosomal calcium mobilization. In other words, intracellular calcium mobilization is a consequence of the activation of PLCε. To confirm this view, we performed experiments similar to those summarized in Fig. S2B, but substituting the TAT-cAMP sponge by anti- PLCε antibodies. In the dark, NP-EGTA is active, chelates intra-acrosomal calcium and maintains it temporarily unavailable. Thus, initiating the AR with external calcium in sperm loaded with the photosensitive chelator puts the exocytotic cascade into motion. The cascade, however, cannot advance beyond the stage when intra-acrosomal calcium is required unless the chelator is destroyed by illumination. Sequestration of PLCε after challenging NP-EGTA-AM-loaded sperm with external calcium did not prevent the AR resumed by UV light. We interpret these findings as indicative that, before we added the antibody, external calcium had triggered a cascade that activated PLCε. As a consequence, PLCε hydrolyzed PIP_2 to generate IP_3, and this opened IP_3-sensitive calcium channels in the acrosomal membrane. When the photosensitive intra-acrosomal calcium chelator was destroyed with UV light, intravesicular calcium was available for release and the AR was resumed (Fig. 6F, black bar). In the control condition, we added anti-PLCε antibodies to sperm loaded with NP-EGTA-AM and incubated for 15 min before treating with external calcium. Under these conditions, the cascade halted at the stage when PLCε should hydrolyze PIP_2, which presumably did not happen because somehow the antibodies prevented the reaction. Thus, there was no IP_3, no opening of sensitive channels and therefore no AR after destroying NP-EGTA with UV light (Fig. 6F, NP → anti-PLCε → calcium → hν). These results suggest that the role of PLCε in the AR is to catalyze a step upstream calcium mobilization from the acrosome.

3.8. Rap1 and PLCε connect cAMP/Epac to intra-acrosomal calcium mobilization

As stated above, we hypothesize that IP_3 generated by hydrolysis of PIP_2 by PLCε drives the intracellular calcium mobilization required for the AR. If this was the case, then anti-PLCε antibodies blocked exocytosis because they prevented calcium mobilization. The predictions extend to Rap1, which operates between Epac and PLCε. We scrutinized intracellular calcium mobilization directly by single-cell confocal microscopy using the fluorescent sensor Fluo3-AM as described earlier. The activation of Epac with the selective analog 8-pCPT-2′-*O*-Me-cAMP induced the efflux of calcium from the acrosome in SLO-permeabilized sperm (Figs. 5B, 7A and S3C). Preincubation with anti-Rap1 antibodies prevented it (Fig. 7B). Loading SLO-permeabilized sperm with U73122 (Fig. 7C) or anti-PLCε antibodies (Fig. 7D) abolished the capacity of the Epac activator to mobilize intracellular calcium. Used at the same concentration as anti-PLCε, anti-PLCγ1 antibodies did not interfere with calcium mobilization (Fig. S3D). These findings lend further support to the view that the effect of the anti-PLCε antibodies is specific. Taken together, our results suggest that cAMP/Epac/Rap1/PLCε/IP_3 constitute a signaling module that governs the intravesicular calcium mobilization essential for sperm exocytosis. A diagram illustrating our current molecular model for the AR that highlights the findings reported here is supplied in Fig. 8.

4. Discussion

An influx of calcium into the cytosol through channels in the plasma membrane almost universally triggers the fusion of secretory vesicles with the cell membrane. Frequently, calcium mobilized from internal sources is also necessary for exocytosis (see Section 1). The sperm model is ideally suited to address the question of how does cAMP connect to calcium mobilization because (i) exocytosis can proceed in the absence of external calcium (which eliminates potentially confounding recordings), (ii) the acrosome itself is a reservoir of releasable calcium, and (iii) sperm do not undergo any trafficking processes other than exocytosis.

The overexpression of proteins and ablation or silencing of genes that encode them are widely used in the exocytosis field. In sperm, however, only pre-made proteins can be delivered to the intracellular compartments through artificial pores or coupled to cell permeable peptides. We have used both technologies to generate the data presented here. Cell-penetrating peptides, also known as protein transduction domains, efficiently transport cargo inside living cells [4]. Typically, protein transduction domains, such as TAT from AIDS virus, are rich in basic residues [27]. The delivery of a permeant version of Rab3A to live human sperm pioneered the application of this technique in gametes [34]. A screening of the incorporation of several cell-penetrating peptides into sperm was recently published [28]. Here we describe a cAMP buffer that penetrates into human sperm thanks to this mechanism and abolishes cAMP-mediated functions because it captures the endogenous second messenger from the cytosol. The TAT-cAMP sponge inhibits the AR triggered by progesterone in a dose–response fashion (Fig. 2A). The response to progesterone was abolished by 100 nM TAT-cAMP sponge, the same concentration that prevented calcium-triggered AR in SLO-permeabilized sperm (Fig. S2A). These observations suggest that transduction of the TAT-cAMP sponge across the plasma membrane in non-permeabilized sperm was at least as efficient and quantitative as was its diffusion in permeabilized cells. Although it was expected that the sponge permeated into the entire sperm cell, it appears to have accumulated mainly in the acrosomal region (Fig. 1D). Interestingly, this localization coincides with that described for the endogenous RIβ subunit in bovine sperm [64]. The TAT-cAMP sponge cannot bind sperm AKAPs because it lacks the amino-terminal D2 domain essential for such interaction [50], nor can it bind (amino acids 94–169 and 236–244) or inhibit (amino acids 94–97) the catalytic subunit because it lacks the initial amino acids required for the R-C interaction [59]. Thus, we conclude that the effect of the TAT-cAMP sponge is due to its capacity to sequester endogenous cAMP. Direct evidence in support of this mechanism comes from the experiments summarized in Fig. 2C, where we show that the inhibitory effect of the sponge is abolished by saturating it with cAMP.

Both progesterone and the calcium ionophore A23187 rely on the synthesis of cAMP by sAC to elicit exocytosis in human sperm (Fig. 2E-H and [8,60]). We had reported earlier that digestion of endogenous cAMP with recombinant cAMP-specific phosphodiesterase 4D [9] or inhibition of its synthesis with the sAC blocker KH7 [8] prevents calcium from accomplishing the AR in SLO-permeabilized sperm. A comparison with results obtained with sAC $^{-/-}$ mouse sperm are discussed in a previous publication [8]. It has been proposed that sAC synthesizes cAMP in the tail and that this cAMP binds PKA to elicit the protein phosphorylation events that correlate with capacitation in mouse [65] and human [3] sperm. A transmembrane AC would be responsible for the synthesis of cAMP in the mouse sperm head. Blocking this activity with SQ22536 does not prevent the AR triggered by A23187 [65]. Unfortunately, KH7 was not tested in the mouse studies, and therefore whether the apparent discrepancies with the human are due to different models or to some other reason cannot be ascertained with the information currently available. In any case, what we know beyond any doubt is that sperm exocytosis elicited by all inducers tested, notably progesterone, requires cAMP.

Cyclic AMP modulates exocytosis in secretory cells by PKA-dependent and/or PKA-independent mechanisms, the latter are mediated by Epacs. In human sperm, calcium-induced AR is mediated by cAMP/Epac and independent of PKA [9]. Raps (Rap1a, b and Rap2a, b, c) are small molecular weight GTPases of the Ras family. Raps serve as substrates for Epac's enzymatic activity. The presence and localization of Epac and Rap isoforms in mammalian sperm has been recently reviewed [61]. A large body of evidence shows that the signaling module cAMP/Epac/Rap governs many biological responses in a variety of cells. Yet its relevance in regulated exocytosis has only been scrutinized in a handful of studies: Epac2A/Rap1 are required for cAMP/Epac-dependent potentiation of insulin secretion [19,55] and intracellular

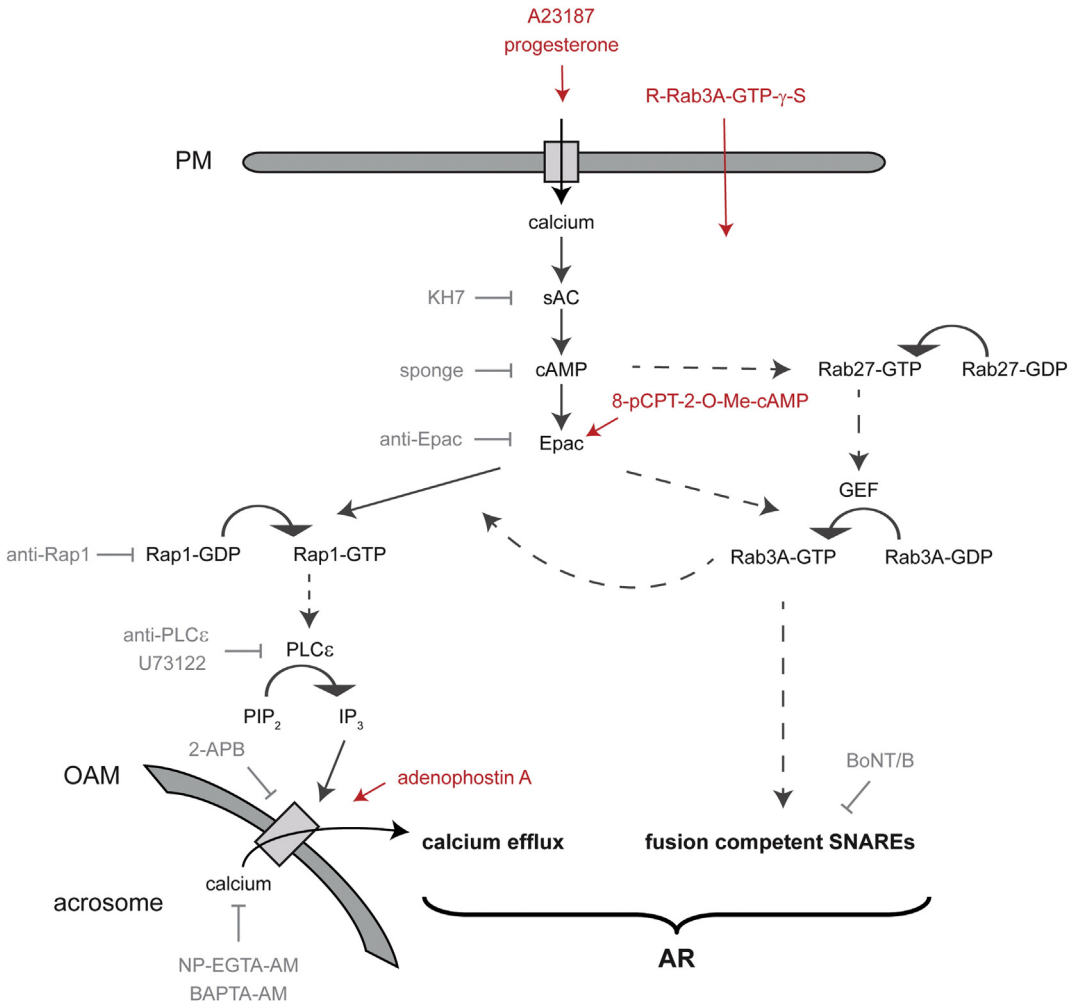

Fig. 8. Updated working model for the AR. Calcium enters the cell from the extracellular milieu through calcium channels opened in response to progesterone, through the SLO-generated pores or is transported by the calcium ionophore A23187. Downstream this calcium we find sAC, which converts ATP into cAMP. Cyclic AMP synthesized by sAC activates Epac and here the signaling pathway splits into two limbs. In one of them, Epac catalyzes the exchange of GDP for GTP on Rap1. In the other, secretory Rabs are activated. Rap1-GTP heads a pathway that leads to acrosomal calcium mobilization. This pathway includes, but is not restricted to, a PLCε and its reaction product IP_3 ("calcium efflux" in the Figure). Rab27-GTP heads a pathway that leads to the correct assembly of the fusion machinery. This pathway includes the exchange of GDP for GTP on Rab3 and several other reactions not represented in the diagram for simplicity ("fusion competent SNAREs" in the Figure). Rab3A-GTP connects both pathways by activating Rap1 on the other limb. The step catalyzed by active SNAREs converges with the local increase in calcium coming from the acrosome downstream of Rap1-GTP/PLCε/IP_3 to accomplish the final steps of membrane fusion ("AR" in the Figure). AR blockers used in this manuscript are shown in light gray. Adenophostin A (red) binds IP_3-sensitive channels and mobilizes acrosomal calcium pharmacologically. Also in red are the AR inducers progesterone, A23187, R-Rab3A-GTPγ-S, and 8-pCPT-2′-*O*-Me-cAMP. PM, plasma membrane; OAM, outer acrosomal membrane. Solid arrows mean there is one step between the terms connected, dashed arrows mean that the number of steps is either unknown or not depicted for simplicity. Modified from Ruete et al. [47].

calcium mobilization [18]. Epac1/Rap1 are required for pancreatic amylase [48] and non-amyloidogenic-soluble form of the amyloid precursor protein α [36] release. Epac1/Rap2 contribute to chlorine secretion in human intestinal epithelial cells [24]. Epac/Rap1 control cAMP-mediated exocytosis of Weibel–Palade bodies in endothelial cells [62] and the secretion of hepatic FGF21 elicited by glucagon [15]. The AR elicited by 8-pCPT-2′-*O*-Me-cAMP, recombinant Rab3A-GTP-γ-S, and calcium requires endogenous, active Rap1. The amount of Rap1-GTP pulled down from cells challenged with 8-pCPT-2′-*O*-Me-cAMP in human (50 μM, 15 min, [8]), mouse (500 μM, 15 min, [2]), and boar (50 μM, 2 h, [38]) sperm is substantially higher than that from untreated controls. Active Rap1 localizes to the acrosomal region upon challenging SLO-permeabilized sperm with calcium [47]. Here we show that progesterone and A23187 augment the percentage of non-permeabilized sperm cells exhibiting acrosomal Rap1-GTP (Fig. 3A, B, E). Activation requires cAMP (Fig. 3B) but not PKA (Fig. 3E). The stimulation of Epac with 8-pCPT-2′-*O*-Me-cAMP is sufficient to achieve Rap1 activation in a high percentage of sperm (Fig. 3E). Recombinant R-Rab3A-GTP-γ-S promotes the exchange of GDP for GTP on Rap1 (Fig. S1) and the AR (Fig. 2D) in a cAMP-dependent manner. In the last few years, it became appreciated that Rap1 proteins serve in interconnected signaling networks [36,44]. The only references to a possible connectivity between Rabs3 or 27 with Rap1 are indirect insofar as they describe the interactions between Rap1GAP2 and the Rab27 effectors synaptotagmin-like protein 1 [40] and 2 [67]. Here we presented direct evidence of the connection between Rab3A and Rap1 during secretion. The pathway appears to be unidirectional because Rap1 is not required to exchange GDP for GTP on Rab3 [8].

External calcium is dispensable for the AR elicited by cAMP [9], recombinant Rab3A [16,34], Arf6 [41], and diacylglycerol [35], but internal calcium is not. Nevertheless, intracellular calcium mobilization alone does not trigger secretion. In sperm with their plasma membrane permeabilized with SLO, cAMP, but not PKA, is required to mobilize calcium from the granule (Figs. 4 and 5). One important caveat to the interpretation of findings obtained using PKA inhibitors is that they can only establish PKA-independence but cannot definitively establish a role for

Epac. Here we present direct evidence that cAMP/Epac/Rap1 mobilize calcium from the acrosome because the stimulation of sperm's Epac with 8-pCPT-2′-*O*-Me-cAMP suffices to elicit intra-acrosomal calcium efflux shortly after the application (Fig. 5B). Anti-Epac (Fig. 5C) and anti-Rap1 (Fig. 7B) antibodies antagonize this effect. Intravesicular calcium mobilization exhibits a lag time that is not due to the kinetics of cAMP diffusion. First, we took great care in mixing the drugs with the bathing solution rapidly to accomplish homogeneous concentration. Second, cells were permeabilized with SLO so that access to the cytosolic compartment was not slowed by diffusion across the plasma membrane. Thus, the delay must reflect the latency of signaling events downstream of Epac. Unlike excitable cells, sperm do not have their secretory granules in close proximity to the plasma membrane primed for immediate exocytosis. Instead, the initiation of exocytosis must accomplish the activation of the fusion machinery and concomitant approximation of the acrosome to the plasma membrane achieved via swelling of the acrosomal contents followed by docking. Swelling is cAMP dependent (Fig. 2E-H) and rate limiting [57].

In SLO-permeabilized human sperm, the AR elicited by calcium, persistently active Arf6 [41] and Rab3A, 8-pCPT-2′-*O*-Me-cAMP [8], diacylglycerol and a non-hydrolyzable analog [35], is sensitive to the PLC blocker U73122. Furthermore, 8-pCPT-2′-*O*-Me-cAMP elicits a calcium signal in non-permeabilized sperm; this signal is abrogated by U73122 [8]. Here, we moved several steps forward and identified the presence and localization of the ε isoform of PLC in human sperm (Fig. 6A). PLCε is required for the AR triggered by calcium and 8-pCPT-2′-*O*-Me-cAMP (Fig. 6B, C). Furthermore, 8-pCPT-2′-*O*-Me-cAMP failed to mobilize intra-acrosomal calcium in sperm treated with U73122 (Fig. 7C) or anti-PLCε antibodies (Fig. 7D). Likewise, experiments conducted with pancreatic islets from PLCε$^{-/-}$ mice demonstrated the requirement of this enzyme downstream of Epac2/Rap1 for the potentiation of glucose-induced insulin release and intracellular calcium mobilization [18,19]. There is also pharmacological evidence of the requirement of a PLC for Epac1/Rap2-regulated chlorine secretion in human intestinal epithelial cells [24]. Thus, it is tempting to interpret the relationship between Epac, Rap1, and PLCε as molecular links between the two universal second messengers calcium and cAMP.

5. Conclusions

Our findings indicate that Epac activation by cAMP leads to the exchange of GDP for GTP on Rap1 in the acrosomal region of the sperm, with the subsequent recruitment and/or activation of a PLCε activity. This enzyme hydrolyzes PIP_2 to generate IP_3, which binds IP_3-sensitive channels and promotes the release of calcium stored in the acrosomal granule. cAMP also mediates the activation of endogenous Rabs 3 and 27, mandatory events in the exocytotic cascade. The efflux of calcium from the acrosome and the assembly of the fusion machinery converge to accomplish the fusion of the acrosome to the plasma membrane (Fig. 8). The contribution of this paper to the sperm biology field is the characterization of signaling pathways through which the physiological trigger progesterone achieves the AR; of particular relevance is the finding that it requires endogenous cAMP and three small GTPases. The contribution of this paper to the exocytosis field is to have generated direct evidence for the role of each and every component of the signaling module cAMP/Epac/Rap1/PLCε in dense-core granule secretion.

Supplementary data to this article can be found online at http://dx.doi.org/10.1016/j.bbamcr.2015.12.007.

Funding

This work was supported by grants from Agencia Nacional de Promoción Científica y Tecnológica (PICT2010-0342, Argentina) and Secretaría de Ciencia y Técnica-Universidad Nacional de Cuyo (grant number 06/J416, Argentina) to C.N.T.

Conflict of interest

None declared.

Transparency document

The Transparency document associated with this article can be found, in the online version.

Acknowledgements

The authors thank M. Furlán, A. Medero, E. Bocanegra, N. Domizio, and J. Ibáñez for excellent technical assistance, and Drs. Binz, Coso, Lopez, Regazzi, and Shirakawa for plasmids. Drs. L. Mayorga and S. Moreno are acknowledged for revising this manuscript critically for important intellectual content.

References

[1] F. Ackermann, N. Zitranski, D. Heydecke, B. Wilhelm, T. Gudermann, I. Boekhoff, The multi-PDZ domain protein MUPP1 as a lipid raft-associated scaffolding protein controlling the acrosome reaction in mammalian spermatozoa, J. Cell. Physiol. 214 (2008) 757.
[2] R. Amano, J. Lee, N. Goto, H. Harayama, Evidence for existence of cAMP-Epac signaling in the heads of mouse epididymal spermatozoa, J. Reprod. Dev. 53 (2007) 127.
[3] M.A. Battistone, R. Da, V, A.M. Salicioni, F.A. Navarrete, D. Krapf, P.E. Visconti, P.S. Cuasnicu, Functional human sperm capacitation requires both bicarbonate-dependent PKA activation and down-regulation of Ser/Thr phosphatases by Src family kinases, Mol. Hum. Reprod. 19 (2013) 570.
[4] C. Bechara, S. Sagan, Cell-penetrating peptides: 20 years later, where do we stand? FEBS Lett. 587 (2013) 1693.
[5] J.L. Bos, Epac: a new cAMP target and new avenues in cAMP research, Nat. Rev. Mol. Cell Biol. 4 (2003) 733.
[6] J.L. Bos, Epac proteins: multi-purpose cAMP targets, Trends Biochem. Sci. 31 (2006) 680.
[7] J.L. Bos, H. Rehmann, A. Wittinghofer, GEFs and GAPs: critical elements in the control of small G proteins, Cell 129 (2007) 865.
[8] M.T. Branham, M.A. Bustos, G.A. De Blas, H. Rehmann, V.E. Zarelli, C.L. Trevino, A. Darszon, L.S. Mayorga, C.N. Tomes, Epac activates the small G proteins Rap1 and Rab3A to achieve exocytosis, J. Biol. Chem. 284 (2009) 24825.
[9] M.T. Branham, L.S. Mayorga, C.N. Tomes, Calcium-induced acrosomal exocytosis requires cAMP acting through a protein kinase a-independent, Epac-mediated pathway, J. Biol. Chem. 281 (2006) 8656.
[10] R.D. Burgoyne, A. Morgan, Secretory granule exocytosis, Physiol. Rev. 83 (2003) 581.
[11] M.A. Bustos, O. Lucchesi, M.C. Ruete, L.S. Mayorga, C.N. Tomes, Rab27 and Rab3 sequentially regulate human sperm dense-core granule exocytosis, Proc. Natl. Acad. Sci. U. S. A. 109 (2012) E2057–E2066.
[12] X. Cheng, Z. Ji, T. Tsalkova, F. Mei, Epac and PKA: a tale of two intracellular cAMP receptors, Acta Biochim. Biophys. Sin. 40 (2008) 651 (Shanghai).
[13] T. Coppola, V. Perret-Menoud, S. Gattesco, S. Magnin, I. Pombo, U. Blank, R. Regazzi, The death domain of Rab3 guanine nucleotide exchange protein in GDP/GTP exchange activity in living cells, Biochem. J. 362 (2002) 273.
[14] S. Costello, F. Michelangeli, K. Nash, L. Lefievre, J. Morris, G. Hado-Oliveira, C. Barratt, J. Kirkman-Brown, S. Publicover, Ca^{2+}-stores in sperm: their identities and functions, Reproduction 138 (2009) 425.
[15] H.A. Cyphert, K.M. Alonge, S.M. Ippagunta, F.B. Hillgartner, Glucagon stimulates hepatic FGF21 secretion through a PKA- and EPAC-dependent posttranscriptional mechanism, PLoS ONE 9 (2014), e94996.
[16] G. De Blas, M. Michaut, C.L. Trevino, C.N. Tomes, R. Yunes, A. Darszon, L.S. Mayorga, The intraacrosomal calcium pool plays a direct role in acrosomal exocytosis, J. Biol. Chem. 277 (2002) 49326.
[17] J. de Rooij, F.J. Zwartkruis, M.H. Verheijen, R.H. Cool, S.M. Nijman, A. Wittinghofer, J.L. Bos, Epac is a Rap1 guanine-nucleotide-exchange factor directly activated by cyclic AMP, Nature 396 (1998) 474.
[18] I. Dzhura, O.G. Chepurny, G.G. Kelley, C.A. Leech, M.W. Roe, E. Dzhura, P. Afshari, S. Malik, M.J. Rindler, X. Xu, Y. Lu, A.V. Smrcka, G.G. Holz, Epac2-dependent mobilization of intracellular Ca^{2+} by glucagon-like peptide-1 receptor agonist exendin-4 is disrupted in beta-cells of phospholipase C-epsilon knockout mice, J. Physiol. 588 (2010) 4871.
[19] I. Dzhura, O.G. Chepurny, C.A. Leech, M.W. Roe, E. Dzhura, X. Xu, Y. Lu, F. Schwede, H.G. Genieser, A.V. Smrcka, G.G. Holz, Phospholipase C-epsilon links Epac2 activation to the potentiation of glucose-stimulated insulin secretion from mouse islets of Langerhans, Islets 3 (2011) 121.
[20] A. Finkelstein, J. Zimmerberg, F.S. Cohen, Osmotic swelling of vesicles: its role in the fusion of vesicles with planar phospholipid bilayer membranes and its possible role in exocytosis, Annu. Rev. Physiol. 48 (1986) 163.
[21] B. Franke, J.W. Akkerman, J.L. Bos, Rapid Ca^{2+}-mediated activation of Rap1 in human platelets, EMBO J. 16 (1997) 252.
[22] M. Gloerich, J.L. Bos, Epac: defining a new mechanism for cAMP action, Annu. Rev. Pharmacol. Toxicol. 50 (2010) 355.

[23] C.W. Gourlay, K.R. Ayscough, Actin-induced hyperactivation of the Ras signaling pathway leads to apoptosis in Saccharomyces cerevisiae, Mol. Cell. Biol. 26 (2006) 6487.
[24] K.M. Hoque, O.M. Woodward, D.B. van Rossum, N.C. Zachos, L. Chen, G.P. Leung, W.B. Guggino, S.E. Guggino, C.M. Tse, Epac1 mediates protein kinase A-independent mechanism of forskolin-activated intestinal chloride secretion, J. Gen. Physiol. 135 (2010) 43.
[25] X.Q. Hu, S.Y. Ji, Y.C. Li, C.H. Fan, H. Cai, J.L. Yang, C.P. Zhang, M. Chen, Z.F. Pan, Z.Y. Hu, F. Gao, Y.X. Liu, Acrosome formation-associated factor is involved in fertilization, Fertil. Steril. 93 (2010) 1482.
[26] D.M. Hutt, J.M. Baltz, J.K. Ngsee, Synaptotagmin VI and VIII and syntaxin 2 are essential for the mouse sperm acrosome reaction, J Biol Chem. 280 (2005) 20197.
[27] A. Joliot, A. Prochiantz, Transduction peptides: from technology to physiology, Nat. Cell Biol. 6 (2004) 189.
[28] S. Jones, M. Lukanowska, J. Suhorutsenko, S. Oxenham, C. Barratt, S. Publicover, D.M. Copolovici, U. Langel, J. Howl, Intracellular translocation and differential accumulation of cell-penetrating peptides in bovine spermatozoa: evaluation of efficient delivery vectors that do not compromise human sperm motility, Hum. Reprod. 28 (2013) 1874.
[29] H. Kawasaki, G.M. Springett, N. Mochizuki, S. Toki, M. Nakaya, M. Matsuda, D.E. Housman, A.M. Graybiel, A family of cAMP-binding proteins that directly activate Rap1, Science 282 (1998) 2275.
[30] B.J. Kim, K.H. Park, C.Y. Yim, S. Takasawa, H. Okamoto, M.J. Im, U.H. Kim, Generation of nicotinic acid adenine dinucleotide phosphate and cyclic ADP-ribose by glucagon-like peptide-1 evokes Ca^{2+} signal that is essential for insulin secretion in mouse pancreatic islets, Diabetes 57 (2008) 868.
[31] H. Kondo, R. Shirakawa, T. Higashi, M. Kawato, M. Fukuda, T. Kita, H. Horiuchi, Constitutive GDP/GTP exchange and secretion-dependent GTP hydrolysis activity for Rab27 in platelets, J. Biol. Chem. 281 (2006) 28657.
[32] C.A. Leech, O.G. Chepurny, G.G. Holz, Epac2-dependent rap1 activation and the control of islet insulin secretion by glucagon-like peptide-1, Vitam. Horm. 84 (2010) 279.
[33] K. Lefkimmiatis, M.P. Moyer, S. Curci, A.M. Hofer, "cAMP sponge": a buffer for cyclic adenosine 3′, 5′-monophosphate, PLoS ONE 4 (2009), e7649.
[34] C.I. Lopez, S.A. Belmonte, G.A. De Blas, L.S. Mayorga, Membrane-permeant Rab3A triggers acrosomal exocytosis in living human sperm, FASEB J. 21 (2007) 4121.
[35] C.I. Lopez, L.E. Pelletan, L. Suhaiman, G.A. De Blas, N. Vitale, L.S. Mayorga, S.A. Belmonte, Diacylglycerol stimulates acrosomal exocytosis by feeding into a PKC- and PLD1-dependent positive loop that continuously supplies phosphatidylinositol 4,5-bisphosphate, Biochim. Biophys. Acta 1821 (2012) 1186.
[36] M. Maillet, S.J. Robert, M. Cacquevel, M. Gastineau, D. Vivien, J. Bertoglio, J.L. Zugaza, R. Fischmeister, F. Lezoualc'h, Crosstalk between Rap1 and Rac regulates secretion of sAPP alpha, Nat. Cell Biol. 5 (2003) 633.
[37] C. Mendoza, A. Carreras, J. Moos, J. Tesarik, Distinction between true acrosome reaction and degenerative acrosome loss by a one-step staining method using *Pisum sativum* agglutinin, J. Reprod. Fertil. 95 (1992) 755.
[38] A. Miro-Moran, I. Jardin, C. Ortega-Ferrusola, G.M. Salido, F.J. Pena, J.A. Tapia, I.M. Aparicio, Identification and function of exchange proteins activated directly by cyclic AMP (Epac) in mammalian spermatozoa, PLoS ONE 7 (2012), e37713.
[39] K.J. Mitchell, F.A. Lai, G.A. Rutter, Ryanodine receptor type I and nicotinic acid adenine dinucleotide phosphate receptors mediate Ca^{2+} release from insulin-containing vesicles in living pancreatic β-cells (MIN6), J. Biol. Chem. 278 (2003) 11057.
[40] O. Neumuller, M. Hoffmeister, J. Babica, C. Prelle, K. Gegenbauer, A.P. Smolenski, Synaptotagmin-like protein 1 interacts with the GTPase-activating protein Rap1GAP2 and regulates dense granule secretion in platelets, Blood 114 (2009) 1396.
[41] L.E. Pelletan, L. Suhaiman, C.C. Vaquer, M.A. Bustos, G.A. De Blas, N. Vitale, L.S. Mayorga, S.A. Belmonte, ADP ribosylation factor 6 (ARF6) promotes acrosomal exocytosis by modulating lipid turnover and Rab3A activation, J. Biol. Chem. 290 (2015) 9823.
[42] C.A. Pocognoni, G.A. De Blas, A.P. Heuck, S.A. Belmonte, L.S. Mayorga, Perfringolysin O as a useful tool to study human sperm physiology, Fertil. Steril. 99 (2013) 99.
[43] S. Publicover, C.V. Harper, C. Barratt, $[Ca^{2+}]_i$ signalling in sperm–making the most of what you've got, Nat. Cell Biol. 9 (2007) 235.
[44] J.H. Raaijmakers, J.L. Bos, Specificity in ras and rap signaling, J. Biol. Chem. 284 (2009) 10995.
[45] H. Rehmann, J. Das, P. Knipscheer, A. Wittinghofer, J.L. Bos, Structure of the cyclic-AMP-responsive exchange factor Epac2 in its auto-inhibited state, Nature 439 (2006) 625.
[46] F. Rodriguez, M.A. Bustos, M.N. Zanetti, M.C. Ruete, L.S. Mayorga, C.N. Tomes, alpha-SNAP prevents docking of the acrosome during sperm exocytosis because it sequesters monomeric syntaxin, PLoS ONE 6 (2011), e21925.
[47] M.C. Ruete, O. Lucchesi, M.A. Bustos, C.N. Tomes, Epac, rap and Rab3 act in concert to mobilize calcium from sperm inverted question marks acrosome during exocytosis, Cell Commun. Signal. 12 (2014) 43.
[48] M.E. Sabbatini, X. Chen, S.A. Ernst, J.A. Williams, Rap1 activation plays a regulatory role in pancreatic amylase secretion, J. Biol. Chem. 283 (2008) 23884.
[49] C. Sanchez-Cardenas, M.R. Servin-Vences, O. Jose, C.L. Trevino, A. Hernandez-Cruz, A. Darszon, Acrosome reaction and Ca^{2+} imaging in single human spermatozoa: new regulatory roles of $[Ca^{2+}]_i$, Biol. Reprod. 91 (2014) 67.
[50] G.N. Sarma, F.S. Kinderman, C. Kim, D.S. Von, L. Chen, B.C. Wang, S.S. Taylor, Structure of D-AKAP2:PKA RI complex: insights into AKAP specificity and selectivity, Structure 18 (2010) 155.
[51] M. Schmidt, F.J. Dekker, H. Maarsingh, Exchange protein directly activated by cAMP (Epac): a multidomain cAMP mediator in the regulation of diverse biological functions, Pharmacol. Rev. 65 (2013) 670.
[52] N. Schultz, F.K. Hamra, D.L. Garbers, A multitude of genes expressed solely in meiotic or postmeiotic spermatogenic cells offers a myriad of contraceptive targets, Proc. Natl. Acad. Sci. U. S. A. 100 (2003) 12201.
[53] S. Seino, Cell signalling in insulin secretion: the molecular targets of ATP, cAMP and sulfonylurea, Diabetologia 55 (2012) 2096.
[54] S. Seino, T. Shibasaki, PKA-dependent and PKA-independent pathways for cAMP-regulated exocytosis, Physiol. Rev. 85 (2005) 1303.
[55] T. Shibasaki, H. Takahashi, T. Miki, Y. Sunaga, K. Matsumura, M. Yamanaka, C. Zhang, A. Tamamoto, T. Satoh, J. Miyazaki, S. Seino, Essential role of Epac2/Rap1 signaling in regulation of insulin granule dynamics by cAMP, Proc. Natl. Acad. Sci. U. S. A. 104 (2007) 19333.
[56] A.V. Smrcka, J.H. Brown, G.G. Holz, Role of phospholipase Cε in physiological phosphoinositide signaling networks, Cell. Signal. 24 (2012) 1333.
[57] C.M. Sosa, M.A. Pavarotti, M.N. Zanetti, F.C. Zoppino, G.A. De Blas, L.S. Mayorga, Kinetics of human sperm acrosomal exocytosis, Mol. Hum. Reprod. 21 (2015) 244.
[58] M. Szaszak, F. Christian, W. Rosenthal, E. Klussmann, Compartmentalized cAMP signalling in regulated exocytic processes in non-neuronal cells, Cell. Signal. 20 (2008) 590.
[59] S.S. Taylor, C. Kim, D. Vigil, N.M. Haste, J. Yang, J. Wu, G.S. Anand, Dynamics of signaling by PKA, Biochim. Biophys. Acta 1754 (2005) 25.
[60] M.E. Teves, H.A. Guidobaldi, D.R. Unates, R. Sanchez, W. Miska, S.J. Publicover, A.A. Morales Garcia, L.C. Giojalas, Molecular mechanism for human sperm chemotaxis mediated by progesterone, PLoS ONE 4 (2009), e8211.
[61] C.N. Tomes, The proteins of exocytosis: lessons from the sperm model, Biochem. J. 465 (2015) 359.
[62] K.W. van Hooren, E.L. van Agtmaal, M. Fernandez-Borja, J.A. van Mourik, J. Voorberg, R. Bierings, The Epac-Rap1 signaling pathway controls cAMP-mediated exocytosis of Weibel–Palade bodies in endothelial cells, J. Biol. Chem. 287 (2012) 24713.
[63] M. van Triest, J.L. Bos, Pull-down assays for guanoside 5′-triphosphate-bound Ras-like guanosine 5′-triphosphatases, Methods Mol. Biol. 250 (2004) 97.
[64] S. Vijayaraghavan, G.E. Olson, S. NagDas, V.P. Winfrey, D.W. Carr, Subcellular localization of the regulatory subunits of cyclic adenosine 3′,5′-monophosphate-dependent protein kinase in bovine spermatozoa, Biol. Reprod. 57 (1997) 1517.
[65] E. Wertheimer, D. Krapf, J.L. de la Vega-Beltran, C. Sanchez-Cardenas, F. Navarrete, D. Haddad, J. Escoffier, A.M. Salicioni, L.R. Levin, J. Buck, J. Mager, A. Darszon, P.E. Visconti, Compartmentalization of distinct cAMP signaling pathways in mammalian sperm, J. Biol. Chem. 288 (2013) 35307.
[66] S.M. Wu, V. Baxendale, Y. Chen, A.L. Pang, T. Stitely, P.J. Munson, M.Y. Leung, N. Ravindranath, M. Dym, O.M. Rennert, W.Y. Chan, Analysis of mouse germ-cell transcriptome at different stages of spermatogenesis by SAGE: biological significance, Genomics 84 (2004) 971.
[67] T. Yasuda, M. Fukuda, Slp2-a controls renal epithelial cell size through regulation of rap-ezrin signaling independently of Rab27, J. Cell Sci. 127 (2014) 557.
[68] R. Yunes, M. Michaut, C. Tomes, L.S. Mayorga, Rab3A triggers the acrosome reaction in permeabilized human spermatozoa, Biol. Reprod. 62 (2000) 1084.
[69] N. Zanetti, L.S. Mayorga, Acrosomal swelling and membrane docking are required for hybrid vesicle formation during the human sperm acrosome reaction, Biol. Reprod. 81 (2009) 396.